

The Dirac Sea Contribution To The Energy Of An Electroweak String**Martin Groves and Warren B. Perkins,**

*Department Of Physics,
University of Wales Swansea,
Singleton Park,
Swansea, SA2 8PP,
Great Britain.*

Abstract

We present a systematic determination of the order \hbar fermionic energy shift when an electroweak string is perturbed. We show that the combined effect of zero modes, bound states and continuum states is to lower the total fermionic ground state energy of the string when the Higgs instability of the string is excited. The effect of the Dirac sea is thus to destabilise the string. However, this effect can be offset by populating positive energy states. Fermions enhance the stability of an electroweak string with sufficiently populated fermionic bound states.

1. Introduction

The resurrection of interest in electroweak strings, first discovered by Nambu [1], induced by the discovery of the W and Z-string solutions [2] lead to intense research into the properties and potential impact of these objects. Both the W and Z-strings solutions are U(1) Nielsen-Olesen vortices embedded in some U(1) subgroup of the Weinberg-Salam model [3]. Unlike the archetypal Abelian Higgs Nielsen-Olesen vortex and standard GUT vortices, the stability of these embedded strings is not guaranteed by any topological argument. The enlarged field space of the SU(2)xU(1) Salam Weinberg model provides extra directions in field space which allow the construction of continuous, finite energy paths that unwind the string solution. The criterion for the existence of topological strings is that the first homotopy group of the vacuum manifold is non-trivial [4]. The first homotopy group of the three sphere, which is the vacuum manifold of the electroweak theory, is however trivial and therefore the electroweak string solutions are non-topological in nature. This implies that the W and Z-strings are just finite energy solutions to the classical field equations and, at best, electroweak strings could sit at a local minimum of the electroweak energy functional. They would then be separated from, and prevented from decaying into, the trivial vacuum by a finite energy barrier. This barrier would either have to be surmounted or quantum mechanically tunnelled through to destroy the string solution. Alternatively electroweak strings could be local maxima or saddle points of the energy functional, in which case the pure string solutions would be intrinsically unstable. The issue of stability is a question of energetics and depends on the value of the parameters used. Detailed stability analyses of the Z-string have been carried out by two independent sets of authors[5, 6]. Both investigations concluded that the Z-string solution possess modes of instability except in the unphysical region where $\sin^2(\theta_W) \sim 1$. Other investigations[7] imply that the W-string solutions are unstable for all values of the electroweak parameters. W-strings will not be considered any further during the course of this paper.

The instability of electroweak strings for physical values of the Standard Model parameters would tend to imply that electroweak strings are physically insignificant. Had electroweak strings been stable then we would have expected a network of strings to be formed during the electroweak phase transition through the Kibble mechanism. The density of electroweak strings would be lower than their topological counterparts as the vanishing of the electroweak Higgs field at a point does not necessarily imply the existence of a string. Another important difference arises because electroweak strings would tend to form fragments of finite length that are bounded by a monopole anti-monopole pair. As discussed in [8] the inherent contraction of these string fragments within the electroweak theory provide all of the conditions required for electroweak baryogenesis. Although the CP violation in the minimal electroweak theory is too small to account for the observed baryon anti-baryon asymmetry, electroweak string are also expected to

arise in extensions of the minimal electroweak which admit greater CP violation [9].

The stability analysis discussed thus far has focussed on the pure Z-string solutions. It is however possible that the formation of bound states of other particles on the string may have a non-trivial effect on the stability of electroweak strings. Of particular importance for a string like solution is the effect of a finite density of bound states moving along the string. In [10] the authors considered a toy model in which they extended the electroweak theory by adding an extra global U(1) scalar to the bosonic sector of the electroweak theory. They constructed solutions with a finite U(1) charge per unit length of the string and then investigated the stability of the resulting solutions. They found that it was possible to extend the region in which the electroweak string is stable to $\sin^2(\theta_W) \sim 0.47$. Thus the stability of an electroweak string may be enhanced by its interaction with other fields. The stabilising effects of a plasma of scalar particles have also been considered [11].

The authors of [10] rightly point out that, in the context of the electroweak theory, the pertinent particles to consider are the fermions which gain their mass via a Yukawa coupling to the Higgs field. As will be discussed in this paper, the systematic analysis of fermionic states in the electroweak string background is a far more involved task than the analysis of bosonic condensates. The critical difference arises because of the different statistics satisfied by fermions and bosons. Bose-Einstein statistics allow a significant population of the bosonic ground state and hence a classical treatment of this single mode is appropriate. In sharp contrast, the Pauli exclusion principle does not allow a similar classical treatment in the fermionic case and a complete field theoretic analysis is required. Naively, as the fermions gain their mass through a Yukawa coupling to the Higgs field it would be expected that the massive fermions would rather be localised about the centre of the string and prevent the string from decaying in an attempt to maintain their low energy state. The purpose of this paper is to carryout a systematic analysis of fermions in the background of the Z-string. The effects of the fermionic zero mode on the stability of the string was considered in [12, 13] where it is claimed that the fermionic ground state energy makes a negative contribution to the energy of the string and increases the instability. However, we must consider the full Dirac spectrum. It is not clear what effect the infinite number of continuum states have upon string stability and positive energy bound states can only be consistently included if the actual numerical value of the fermionic ground state energy is calculated. Here we present a systematic, quantitative treatment of the fermionic contribution to the energy of the Z-string.

It will be shown that a systematic treatment of fermions in a string background requires a complete field theoretic calculation. Techniques are developed for the computation and renormalisation of the Dirac sea contribution to the energy of the Z-string. Many of the techniques developed have a wider range

of applicability, particularly for determining Dirac sea energies in other 3+1D backgrounds such as the sphaleron. Having shown how the Dirac sea energy can be computed in the Z-string background, the change in this energy is computed when a mode of instability of the Z-string is excited. This determines the contribution of the fermionic ground state to the stability of the Z-string. Having understood the ground state energy it is possible to consistently consider the effects of filled, positive energy bound states on the stability of the string.

In section 2 we review the electroweak string and its stability. A systematic discussion of the semi-classical treatment of fermion-soliton interactions is given in section 3. In this section the origins of the Dirac sea contribution to the fermionic energy of a soliton are demonstrated from a field theoretic point of view and a formal statement of the required calculation is made. In section 4 we review the Dirac equation in the background of the Z-string and derive the whole fermionic spectrum.

The fermionic ground state energy is divergent and its computation requires the use of a regulator and renormalisation scheme. In section 5 the proper time regularisation procedure is applied and an expression for the regulated fermionic energy of the pure Z-string is derived. We present a consistent renormalisation of the regularised fermionic energy in section 7. The appropriate counter terms are derived using the heat kernel expansion.

In order to calculate the fermionic energy, we must sum over all continuum states. This sum is implemented by discretising the continuum, determining momentum shift functions and analytically recovering the continuum. The formalism for this procedure is established in section 6. To demonstrate the consistency of this procedure and highlight its key physical properties, we analyse a core model string in section 8. The core model introduces simplified string profile functions which allow the Dirac equation to be solved analytically and allows significant insight into numerous subtle aspects of the calculation of the fermionic energy to be gained.

The calculation of real physical interest is presented in section 9. We introduce the perturbed string, determine the Dirac spectrum in this background and evaluate the counter terms. We then apply the formalism of sections 5 to 7 to determine the difference between the ground state fermionic energy of the perturbed string and that of the pure Z-string.

Once the change in the fermionic ground state energy has been calculated it is only a small step to add a finite density of positive energy bound states moving along the string. In section 9 we investigate the effect of changing the density of positive energy states upon the stability of the string and discuss the possibility of stabilising the electroweak string.

We conclude with a summary of what has been learned during this investigation and point towards future avenues of research.

2. Strings in the Electroweak Theory

In this section we review the Z-string solution and its stability. The existence of string in the electroweak theory was first proposed by Nambu [1] in 1977. Interest in electroweak string was however resurrected by Vachaspati [2] with the discovery of the Z-string and W-string solutions.

To set notation, we take the purely bosonic sector of the electroweak theory to be defined by the Lagrangian density,

$$L_{Bosonic} = -\frac{1}{4}W_{\mu\nu}^a W^{a\mu\nu} - \frac{1}{4}F_{\mu\nu}F^{\mu\nu} + |D_\mu\Phi|^2 - \lambda(|\Phi|^2 - \eta^2)^2 \quad (1)$$

where,

$$W_{\mu\nu}^a = \partial_\mu W_\nu^a - \partial_\nu W_\mu^a + \hat{g}\epsilon^{abc}W_\mu^b W_\nu^c, \quad (2)$$

$$F_{\mu\nu} = \partial_\mu B_\nu - \partial_\nu B_\mu, \quad (3)$$

$$D_\mu\Phi = \left(\partial_\mu - \frac{i\hat{g}}{2}\sigma^a W_\mu^a - \frac{ig'}{2}B_\mu\right)\Phi, \quad (4)$$

and,

$$\Phi = \begin{pmatrix} \phi_+ \\ \phi_o \end{pmatrix}, \quad (5)$$

is the standard Higgs doublet. The gauge boson mass eigenstates are defined in the usual way,

$$\begin{pmatrix} Z_\mu \\ A_\mu \end{pmatrix} = \begin{pmatrix} \cos\theta_w & -\sin\theta_w \\ \sin\theta_w & \cos\theta_w \end{pmatrix} \begin{pmatrix} W_\mu^3 \\ B_\mu \end{pmatrix}, \quad W_\mu^\pm = \frac{1}{\sqrt{2}}(W_\mu^1 \pm iW_\mu^2), \quad (6)$$

where θ_w is the Weinberg angle, $\hat{g} = 2q \cos\theta_w$ and $g' = 2q \sin\theta_w$.

The Z-string ansatz is defined by [2],

$$Z_1 = -\frac{\nu(r)}{qr} \sin\theta, \quad Z_2 = \frac{\nu(r)}{qr} \cos\theta, \quad \phi_o = \eta f(r)e^{i\theta}, \quad (7)$$

with all other fields in the theory set to zero. By keeping only the fields which are non-zero in the Z-string background, the energy of the field configuration becomes,

$$E = \int d^3x \left(\frac{1}{4}Z_{ij}^2 + |\partial_i\phi_o - iqZ_i\phi_o|^2 + \lambda(|\phi_o|^2 - \eta^2)^2 \right), \quad (8)$$

where the indices $i, j = 1, 2, 3$. Rescaling the radial variable by $r \rightarrow M_z r$, allows the energy per unit length of the string (in units of M_z^2) to be written as,

$$E_{string} = 2\pi \int_0^\infty dr r \left(\left(\frac{\nu'}{r}\right)^2 + (f')^2 + \left(\frac{f}{r}\right)^2 (\nu - 1)^2 + \frac{1}{4}\beta^2(f^2 - 1)^2 \right), \quad (9)$$

where, $\beta = \frac{M_H}{M_Z}$. Variation of (9) with respect to the profile functions $f(r)$ and $\nu(r)$, leads to the familiar Nielsen-Olesen equations [14] for a unit winding number string,

$$f''(r) + \frac{f'(r)}{r} - \frac{f(r)}{r^2}(\nu(r) - 1)^2 - \beta(f(r)^2 - 1)f(r) = 0, \quad (10)$$

$$\nu''(r) - \frac{\nu'(r)}{r} - (\nu(r) - 1)f^2(r) = 0. \quad (11)$$

Thus the Z-string is a $U(1)$ Nielsen-Olesen string embedded in the electroweak theory in the direction of the $U(1)_Z$ subgroup generated by the Z gauge particle. The Z-string is not topologically stable, such a field configuration can decay to the trivial vacuum, and stability is an issue of energetics. By searching the $(\beta, \sin^2 \theta_w)$ plane it is found that the electroweak string is unstable except for $\sin^2 \theta_w \approx 1$ [5, 6]. Of particular importance, electroweak strings are unstable for the physically observed values of the electroweak parameters ($\sin^2 \theta_w \approx 0.23$).

For a unit winding number string two modes of instability were found. The first corresponding to the upper component of the Higgs doublet, ϕ_+ , acquiring a non-zero value in the string core and the second corresponding to the W field,

$$W_{\downarrow}^- = \frac{e^{i\theta}}{\sqrt{2}}(W_r^- + \frac{i}{r}W_{\theta}^-), \quad (12)$$

forming a non-zero value inside the string core. The latter instability corresponds to the formation of a W-condensate inside the string, this mode of instability has been investigated in [15, 16]. The effect of these modes is to cause the string to unwind and decay to the trivial vacuum.

The stability of electroweak string may however be changed by the presence of bound states. Vachaspati and Watkins [10] found that, by coupling the bosonic sector of the electroweak theory to a global complex scalar field, it is possible to significantly enhance the stability of the Z-string solution by the formation of scalar bound states. However, as they point out, the pertinent particles to consider are the fermions of the standard model. As the Higgs field vanishes in the core of the string, fermions which gain their mass from a Yukawa coupling to the Higgs field will be massless inside the string core. Thus naively they would rather reside within the core of the string and resist its dissolution.

While the scalar case can be considered classically, a purely classical analysis is not possible for fermions as their statistics prevent a large occupation number within a given energy state. Consequently a full quantum mechanical treatment is required.

Fermions in the background of the electroweak string have been considered by several authors [17, 12, 13]. However, only the effects of the zero mode states were considered. We present a systematic calculation of the change in the entire fermionic energy brought about by perturbing the Z-string.

3. Fermion-Soliton Interactions and the Dirac Sea

The fermionic part of the electroweak action can be written in the form,

$$i \int d^4x \Psi^\dagger \hat{A}[\Phi, Z_\mu] \Psi \quad (13)$$

where $\hat{A}[\Phi, Z_\mu]$ is some operator which depends upon the background scalar and gauge fields and the fermionic fields are grouped together in the spinor Ψ . The fermionic contribution to the path integral is a Gaussian functional integral over the fermionic fields. For anti-commuting fields this Gaussian functional integral has the standard result [18],

$$\int D[\Psi^\dagger(x, t)] D[\Psi(x, t)] \exp \left(i \int d^4x \Psi^\dagger \hat{A}[\Phi, Z_\mu] \Psi \right) = \text{Det } \hat{A}[\Phi, Z_\mu]. \quad (14)$$

Using (14) it is possible to formally integrate out the fermionic contribution to the action and obtain an effective action which encapsulates the effects of the fermion fields yet only contains explicit dependence on the bosonic fields. This can rarely be done in practice because the calculation of the determinant in (14) requires a knowledge of all the eigenvalues of the operator $\hat{A}[\Phi, Z_\mu]$ for a general background. Instead we consider specific backgrounds.

The operator $\hat{A}[\Phi, Z_\mu]$ is related to the Dirac Hamiltonian $\hat{H}[\Phi, Z_\mu]$ in the bosonic background of the fields Φ and Z_μ by,

$$\hat{A}[\Phi, Z_\mu] = i \frac{\partial}{\partial t} - \hat{H}[\Phi, Z_\mu]. \quad (15)$$

For a static field configuration the Dirac Hamiltonian has the set of energy eigenvalues $\{E_r\}$ which satisfy,

$$\hat{H}[\Phi, Z_\mu] \Psi_r = E_r \Psi_r. \quad (16)$$

This is just the Dirac equation describing the fermions in the background of the string.

The determinant in (14) can be expressed in terms of the energy eigenvalues [18],

$$\text{Det } \hat{A}[\Phi, Z_\mu] = \sum_{\{n_r\}} C(\{n_r\}) \exp \left[-iT \left(\sum_r (-E_r + n_r E_r) \right) \right] \quad (17)$$

where the integers n_r are the occupation numbers of the excited positive energy states and $C(\{n_r\})$ are the associated combinatoric degeneracy factors.

The fermionic ground state energy is then given by,

$$E_{gs} = \sum_r (-E_r). \quad (18)$$

This is exactly the energy which would arise from filling all the negative energy states as predicted by Dirac.

The ground state energy of the field configuration is then given by,

$$E_{ground} = E_{Classical} + \left(E_{bos} + \sum_r (-E_r) \right) \quad (19)$$

where E_{bos} is the effect of the bosonic fluctuations (these will not be considered here).

We will be interested in the difference between the Dirac sea energies of two systems, this will generally be referred to as the fermionic energy difference, which can be written as,

$$\delta E_{fermion} = \sum_{r<0} (E_{r,1} - E_{r,2}), \quad (20)$$

where $E_{r,1}$ and $E_{r,2}$ are the energy eigenvalues of the Dirac operator in the two backgrounds and the sum is over all the negative energy states. It is useful to express the fermionic energy difference (20) as a functional trace over a complete set of eigenfunctions. Specifically,

$$\delta E_{fermion} = -\frac{1}{2} \text{Tr} (|\hat{H}_1| - |\hat{H}_2|) = -\frac{1}{2} \text{Tr} \left(\sqrt{\hat{H}_1^2} - \sqrt{\hat{H}_2^2} \right), \quad (21)$$

where $\hat{H}_{1,2}$ are the Dirac Hamiltonians for the two systems and the factor of $\frac{1}{2}$ arises because the trace in (21) is over both the positive and negative energy eigenstates. These are known to be in a 1 : 1 correspondence through the action of the charge conjugation operator.

The computation of (21) is the aim of this paper. All energies per unit length of string will be expressed in terms of the square of the Higgs VEV.

4. The Dirac Equation in an Electroweak String Background

Fermions enter the electroweak theory through the Lagrangian density,

$$L_{fermion} = i\bar{\Psi}_L \gamma^\mu D_\mu \Psi_L + i\bar{u}_R \gamma^\mu D_\mu u_R + i\bar{d}_R \gamma^\mu D_\mu d_R + L_{Yukawa}, \quad (22)$$

where,

$$L_{Yukawa} = -g_u (\bar{\Psi}_L \tilde{\Phi} u_R + \bar{u}_R \tilde{\Phi}^\dagger \Psi_L) - g_d (\bar{\Psi}_L \Phi d_R + \bar{d}_R \Phi^\dagger \Psi_L), \quad (23)$$

is the Yukawa term which is responsible for generating the masses of the fermions after symmetry breaking.

Φ is the standard Higgs doublet defined by (5) and $\tilde{\Phi}$ is defined to be,

$$\tilde{\Phi} = \begin{pmatrix} \phi_0^* \\ -\phi_+^* \end{pmatrix}.$$

The left handed fermions are combined in the usual $SU(2)$ doublet defined by,

$$\Psi_L = \begin{pmatrix} u_L \\ d_L \end{pmatrix}.$$

The covariant derivatives, which couple the fermions to the gauge fields, are defined by,

$$D_\mu \Psi_L = (\partial_\mu - i\frac{\hat{g}}{2}\sigma^a W_\mu^a - i\frac{g'}{2}Y_L B_\mu)\Psi_L, \quad D_\mu \psi_R = (\partial_\mu - i\frac{g'}{2}Y_R B_\mu)\psi_R,$$

where Y_L and Y_R are the $U(1)_Y$ hypercharges and \hat{g} , g' are the $SU(2)$ and $U(1)_Y$ coupling constants respectively. Throughout explicit reference is made to the up and down quarks through the notation $u_{L,R}$ and $d_{L,R}$. Other fermions can be included by simply introducing the appropriate hypercharges.

Varying the Lagrangian with respect to the fermion fields produces four two component Dirac equations,

$$i\gamma^\mu \partial_\mu u_R - q\alpha_R^u \gamma^\mu Z_\mu u_R + ee^u \gamma^\mu A_\mu u_R - g_u \phi_o u_L + g_u \phi_+ d_L = 0,$$

$$i\gamma^\mu \partial_\mu u_L + q\alpha_L^u \gamma^\mu Z_\mu u_L + ee^u \gamma^\mu A_\mu u_L + e^W \gamma^\mu W_\mu^- d_L - g_u \phi_o^* u_R - g_d \phi_+ d_R = 0,$$

$$i\gamma^\mu \partial_\mu d_R - q\alpha_R^d \gamma^\mu Z_\mu d_R + ee^d \gamma^\mu A_\mu d_R - g_d \phi_+^* u_L - g_d \phi_o^* d_L = 0,$$

$$i\gamma^\mu \partial_\mu d_L + q\alpha_L^d \gamma^\mu Z_\mu d_L + ee^d \gamma^\mu A_\mu d_L + e^W \gamma^\mu W_\mu^+ u_L + g_u \phi_+^* u_R - g_d \phi_o d_R = 0,$$

where, $e = q \sin 2\theta_w$ and $e^W = \sqrt{2}q \cos \theta_w$.

Throughout we use the Weyl representation of the Dirac matrices,

$$\gamma^0 = \begin{pmatrix} 0 & -1 \\ -1 & 0 \end{pmatrix}; \gamma^i = \begin{pmatrix} 0 & \sigma^i \\ -\sigma^i & 0 \end{pmatrix}; \gamma^5 = \gamma_5 \begin{pmatrix} 1 & 0 \\ 0 & 1 \end{pmatrix},$$

with the chiral projection operators defined in the standard way,

$$P_R = \frac{1}{2}(1 + \gamma^5), \quad P_L = \frac{1}{2}(1 - \gamma^5).$$

Working in temporal gauge ($W_o^\pm = A_o = Z_o = 0$) and isolating the time dependence implies that the Dirac equations read,

$$i\partial_t \begin{pmatrix} u_R \\ u_L \\ d_R \\ d_L \end{pmatrix} = \begin{pmatrix} -i\sigma^i D_i^{uR} & -g_u \phi_o & 0 & g_u \phi_+ \\ -g_u \phi_o^* & i\sigma^i D_i^{uL} & -g_d \phi_+ & e^W \sigma^i W_i^- \\ 0 & -g_d \phi_+^* & -i\sigma^i D_i^{dR} & -g_d \phi_o^* \\ g_u \phi_+^* & e^W \sigma^i W_i^+ & -g_d \phi_o & i\sigma^i D_i^{dL} \end{pmatrix} \begin{pmatrix} u_R \\ u_L \\ d_R \\ d_L \end{pmatrix}, \quad (24)$$

where $i = 1, 2, 3$ and the covariant derivatives are defined by,

$$D_i^{PR} = \partial_i + iq\alpha_R^p Z_i - iee^p A_i, \quad D_i^{PL} = \partial_i - iq\alpha_L^p Z_i - iee^p A_i.$$

In the background of the pure Z-string the only non-zero bosonic fields are Z_i (where $i = 1, 2$) and ϕ_o , the specific forms of which are given in (7). The Dirac equation (24) can be seen to decouple into two independent four component equations for the up and down quarks.

As the Z-string solution is independent of z , the Dirac equation in the background of the Z-string can be written as,

$$i\partial_t P - iC\partial_z P = \hat{H}_{2+1,\lambda} P,$$

where P denotes a general 4 component spinor and,

$$C = \begin{pmatrix} -\sigma^3 & 0 \\ 0 & \sigma^3 \end{pmatrix}, \quad \hat{H}_{2+1,\lambda} = \begin{pmatrix} -i\sigma^i D_i^{PR} & -gf(r)e^{i\lambda\theta} \\ -gf(r)e^{-i\lambda\theta} & i\sigma^i D_i^{PL} \end{pmatrix}. \quad (25)$$

$\hat{H}_{2+1,\lambda}$ is the Dirac Hamiltonian defined in the plane perpendicular to the direction of the string. i takes values 1, 2, and the parameter λ allows much of the analysis for the up and down quarks to be carried out using the general Hamiltonian (25), with $\lambda = 1$ for the up quark and -1 for the down quark. The $U(1)_Z$ gauge charges then satisfy,

$$\alpha_L + \alpha_R = \lambda. \quad (26)$$

The parameter λ arises as the left handed up quark couples to ϕ_o and the right handed up quark couples to the complex conjugate field ϕ_o^* , whereas the roles are reversed for the down quark with the left handed component coupling to ϕ_o^* and the right handed component coupling to ϕ_o .

The full 3 + 1D Dirac Hamiltonian can be written as, $\hat{H}_{3+1,\lambda} = \hat{H}_{2+1,\lambda} + iC\partial_z$. Setting,

$$P(\mathbf{x}, t) = P(x_1, x_2)e^{iE_{3+1}t}e^{-ik_z z},$$

where E_{3+1} is the total fermionic energy and k_z is the momentum along the direction of the string, the square of the Dirac equation becomes,

$$E_{3+1,\lambda}^2 P(x_1, x_2) = \hat{H}_{2+1,\lambda}^2 P(x_1, x_2) + k_z^2 P(x_1, x_2),$$

where we have used $\{C, \hat{H}_{2+1,\lambda}\} = 0$. The problem thus reduces to solving the 2 + 1D Dirac equation,

$$E_{2+1,\lambda} P(x_1, x_2) = \hat{H}_{2+1,\lambda} P(x_1, x_2). \quad (27)$$

Using $\{C, \hat{H}_{2+1,\lambda}\} = 0$, if there is a solution of the 2+1 dimensional Dirac equation, $P(x_1, x_2)$, with energy $E_{2+1,\lambda} > 0$ then $CP(x_1, x_2)$ is easily seen to

be a solution with energy $-E_{2+1,\lambda}$. The particle conjugation operator therefore provides a 1 : 1 mapping between the positive and negative energy solutions of the 2 + 1D Dirac equation.

Introducing polar coordinates in the plane perpendicular to the direction of the string, the 2 + 1D Hamiltonian becomes,

$$\hat{H}_{2+1,\lambda} = \begin{pmatrix} 0 & ie^{-i\theta} \begin{pmatrix} -\partial_r + \frac{i}{r}\partial_\theta \\ +\alpha_R \frac{\nu(r)}{r} \end{pmatrix} & -gf(r)e^{i\lambda\theta} & 0 \\ -ie^{i\theta} \begin{pmatrix} \partial_r + \frac{i}{r}\partial_\theta \\ +\alpha_R \frac{\nu(r)}{r} \end{pmatrix} & 0 & 0 & -gf(r)e^{i\lambda\theta} \\ -gf(r)e^{-i\lambda\theta} & 0 & 0 & ie^{-i\theta} \begin{pmatrix} \partial_r - \frac{i}{r}\partial_\theta \\ +\alpha_L \frac{\nu(r)}{r} \end{pmatrix} \\ 0 & -gf(r)e^{-i\lambda\theta} & -ie^{i\theta} \begin{pmatrix} -\partial_r - \frac{i}{r}\partial_\theta \\ +\alpha_L \frac{\nu(r)}{r} \end{pmatrix} & 0 \end{pmatrix}, \quad (28)$$

which acts on a spinor of the form,

$$\Psi_\lambda = \begin{pmatrix} \psi_1^R \\ \psi_2^R \\ \psi_1^L \\ \psi_2^L \end{pmatrix} = \sum_{n=-\infty}^{\infty} \begin{pmatrix} \psi_1(r)e^{in\theta} \\ -i\psi_2(r)e^{i(n+1)\theta} \\ \psi_3(r)e^{i(n-\lambda)\theta} \\ -i\psi_4(r)e^{i(n-\lambda+1)\theta} \end{pmatrix}. \quad (29)$$

The radial profiles of the spinor components are then determined by,

$$(E_{3+1,\lambda} - k_z)\psi_1 = \left(-\partial_r - \frac{n+1}{r} + \alpha_R \frac{\nu(r)}{r} \right) \psi_2 - gf(r)\psi_3, \quad (30)$$

$$(E_{3+1,\lambda} + k_z)\psi_2 = \left(\partial_r - \frac{n}{r} + \alpha_R \frac{\nu(r)}{r} \right) \psi_1 - gf(r)\psi_4, \quad (31)$$

$$(E_{3+1,\lambda} + k_z)\psi_3 = \left(\partial_r + \frac{n-\lambda+1}{r} + \alpha_L \frac{\nu(r)}{r} \right) \psi_4 - gf(r)\psi_1, \quad (32)$$

$$(E_{3+1,\lambda} - k_z)\psi_4 = \left(-\partial_r + \frac{n-\lambda}{r} + \alpha_L \frac{\nu(r)}{r} \right) \psi_3 - gf(r)\psi_2. \quad (33)$$

At small r , the Nielsen Olesen profiles give $f(r) \sim r$ and $\nu(r) \sim r^2$, which give the following small r forms for the spinors,

$$\Psi_1 = r^n \begin{pmatrix} 1 \\ 0 \\ 0 \\ 0 \end{pmatrix}; \Psi_2 = r^{-(n+1)} \begin{pmatrix} 0 \\ 1 \\ 0 \\ 0 \end{pmatrix}; \Psi_3 = r^{(n-\lambda)} \begin{pmatrix} 0 \\ 0 \\ 1 \\ 0 \end{pmatrix}; \Psi_4 = r^{-(n-\lambda+1)} \begin{pmatrix} 0 \\ 0 \\ 0 \\ 1 \end{pmatrix}. \quad (34)$$

At large r , the Nielsen Olesen profiles give $f(r) \sim 1$ and $\nu(r) \sim 1$, which give the following large r forms for the $k_z = 0$ equations of motion,

$$E\psi_1 = -\left(\partial_r + \frac{\nu_\lambda + 1}{r} \right) \psi_2 - g\psi_3, \quad (35)$$

$$E\psi_2 = \left(\partial_r - \frac{\nu_\lambda}{r} \right) \psi_1 - g\psi_4, \quad (36)$$

$$E\psi_3 = \left(\partial_r + \frac{\nu_\lambda + 1}{r} \right) \psi_4 - g\psi_1, \quad (37)$$

$$E\psi_4 = - \left(\partial_r - \frac{\nu_\lambda}{r} \right) \psi_3 - g\psi_2, \quad (38)$$

where,

$$\nu_\lambda = n - \lambda + \alpha_L. \quad (39)$$

The spectrum of states consists of a continuum, bound states and zero modes.

If $E^2 > g^2$, the four linearly independent regular solutions at large r can be expressed in terms of the Bessel functions $J_\nu(z)$ and $N_\nu(z)$,

$$\begin{pmatrix} \psi_1 \\ \psi_2 \\ \psi_3 \\ \psi_4 \end{pmatrix} = a_1 \begin{pmatrix} J_{|\nu_\lambda|}(kr) \\ \mp \frac{E}{k} J_{|\nu_\lambda| \pm 1}(kr) \\ 0 \\ \pm \frac{g}{k} J_{|\nu_\lambda| \pm 1}(kr) \end{pmatrix} + a_2 \begin{pmatrix} 0 \\ \mp \frac{g}{k} J_{|\nu_\lambda| \pm 1}(kr) \\ J_{|\nu_\lambda|}(kr) \\ \pm \frac{E}{k} J_{|\nu_\lambda| \pm 1}(kr) \end{pmatrix} \\ + a_3 \begin{pmatrix} N_{|\nu_\lambda|}(kr) \\ \mp \frac{E}{k} N_{|\nu_\lambda| \pm 1}(kr) \\ 0 \\ \pm \frac{g}{k} N_{|\nu_\lambda| \pm 1}(kr) \end{pmatrix} + a_4 \begin{pmatrix} 0 \\ \mp \frac{g}{k} N_{|\nu_\lambda| \pm 1}(kr) \\ N_{|\nu_\lambda|}(kr) \\ \pm \frac{E}{k} N_{|\nu_\lambda| \pm 1}(kr) \end{pmatrix}, \quad (40)$$

where, $E^2 = k^2 + g^2$, is the usual mass-shell condition. The upper signs correspond to the case when $|\nu_\lambda| = \nu_\lambda$ and the lower signs when $|\nu_\lambda| = -\nu_\lambda$.

If $E^2 < g^2$, the asymptotic radial solutions are modified Bessel functions and the general solution can be written as,

$$\begin{pmatrix} \psi_1 \\ \psi_2 \\ \psi_3 \\ \psi_4 \end{pmatrix} = a_1 \begin{pmatrix} I_{\nu_\lambda}(kr) \\ -\frac{E}{k} I_{\nu_\lambda+1}(kr) \\ 0 \\ \frac{g}{k} I_{\nu_\lambda+1}(kr) \end{pmatrix} + a_2 \begin{pmatrix} 0 \\ -\frac{g}{k} I_{\nu_\lambda+1}(kr) \\ I_{\nu_\lambda}(kr) \\ \frac{E}{k} I_{\nu_\lambda+1}(kr) \end{pmatrix} \\ + a_3 \begin{pmatrix} K_{\nu_\lambda}(kr) \\ \frac{E}{k} K_{\nu_\lambda+1}(kr) \\ 0 \\ -\frac{g}{k} K_{\nu_\lambda+1}(kr) \end{pmatrix} + a_4 \begin{pmatrix} 0 \\ \frac{g}{k} K_{\nu_\lambda+1}(kr) \\ K_{\nu_\lambda}(kr) \\ -\frac{E}{k} K_{\nu_\lambda+1}(kr) \end{pmatrix}, \quad (41)$$

where, $E^2 = g^2 - k^2$, with $k^2 \in (0, g^2)$.

Only the last two independent solutions are square integrable at large r , thus a physical bound state solution must match onto these solutions only.

For each value of n there are two linearly independent, regular short distance spinors, each one matches onto a unique linear combination of the four asymptotic large distance spinors. We denote the matching coefficients by $a_{s,l}$, where $s = 1, 2$ labels the short distance spinor and $l = 1 - 4$ labels the asymptotic spinor. To produce a normalisable state a suitable linear combination of the two regular

short distance spinors must be taken such that the coefficients of the divergent asymptotic solutions are zero. Taking the linear combination, $\alpha\vec{S}_1 + \beta\vec{S}_2$, of the two regular short distance spinors, square integrability implies,

$$\begin{aligned} a_{1,1}\alpha + a_{2,1}\beta &= 0 \\ a_{1,2}\alpha + a_{2,2}\beta &= 0. \end{aligned} \quad (42)$$

A non-trivial solution to (42) exists if and only if the associated determinant is zero, that is,

$$\begin{vmatrix} a_{1,1} & a_{2,1} \\ a_{1,2} & a_{2,2} \end{vmatrix} = 0. \quad (43)$$

In general, finding bound state solutions is reduced to the problem of finding the values of the energy which are roots of (43).

A special case are zero modes [19]. Setting $E = 0$ in the equations of motion, we see that the system decouples into two second order systems for all r .

At small r the leading order behaviour of the two solutions to the first set is given by,

$$\psi_1 \sim r^n, \quad \psi_4 \sim r^{(n+1)} \quad \text{and} \quad \psi_1 \sim r^{-(n-\lambda)}, \quad \psi_4 \sim r^{-(n-\lambda+1)}.$$

While the second system gives,

$$\psi_2 \sim r^{-(n+1)}, \quad \psi_3 \sim r^{-n}, \quad \text{and} \quad \psi_2 \sim r^{(n-\lambda+1)}, \quad \psi_3 \sim r^{(n-\lambda)}.$$

Both systems possess one regular and one irregular asymptotic solution. Thus if both short distance solutions in one system are regular, they will match onto one regular and one irregular asymptotic solution. In the language used above, $a_{1,2} = a_{2,2} = 0$ (say), one constraint is automatically satisfied and there is always a linear combination of short distance spinors that yields a square integrable solution. Thus we have zero mode solutions.

By setting $\lambda = 1$ it is easily seen that the only case in which there are two regular short distance solutions in one system is for $n = 0$. The Up quark zero mode therefore has $n = 0$ and $\psi_2 = \psi_3 = 0$. Further we see we still have a solution to the equations of motion with $\psi_2 = \psi_3 = 0$ if we set $E_{3+1,\lambda} = k_z$. Physically this means that the up quark zero mode can move along the positive direction of the string at the speed of light. This should be compared with the massive bound states which are free to move in either direction along the string. This restriction on the motion of the zero mode has important implications for the formulation of the Dirac sea energy.

Similarly, by setting $\lambda = -1$ we find the only down quark zero mode if $n = -1$. The solution has $\psi_1 = \psi_4 = 0$ and $E_{3+1,\lambda} = -k_z$, thus this mode is restricted to move in the negative z -direction at the speed of light.

The existence of these zero mode solutions in the pure Z-string background is guaranteed by an index theorem [20]. If the string is perturbed, the zero modes

are lifted and become (for small perturbations) low energy massive bound states [12, 13]. The existence of massive bound state solutions is not guaranteed by any form of index theorem but depends upon the precise values of the parameters in the theory. For each set of parameters, solutions to the bound state condition (43) must be searched for.

5. Regulating The Fermionic Energy

We have seen that the fermionic vacuum energy can be calculated by summing over all the negative energy eigenvalues of the Dirac equation in the background of interest. Clearly this quantity is divergent: there are an infinite number of continuum states which make progressively larger contributions to the sum. This problem is closely linked with the usual ultraviolet divergences which arise in quantum field theory when large values of loop momenta are integrated over. Effectively the Dirac sea energy corresponds to a 1-loop calculation in the background of some field configuration. As with normal loop calculations these divergences can be consistently handled using a renormalisation procedure. The issue of regulation is discussed in this section and renormalisation is discussed in section 7.

It is useful to look in a semi-quantitative manner at the nature of the ultraviolet divergences expected. The continuum energy contribution takes the form of an integral over all the momentum components, the nature of the divergences can be isolated by introducing a naive ultraviolet cut-off, Λ ,

$$E_{cont} \sim \int^{\Lambda} d^3k E \sim O(\Lambda^4) + O(\Lambda^2) + O(\log \Lambda) + \dots$$

The first term above will cancel when two strings are compared, leaving quadratic (Λ^2) and logarithmic ($\log \Lambda$) divergences which must be dealt with through the renormalisation procedure.

The freedom to move along the length of the string also means that the bound states contribute to the divergences in the fermionic energy,

$$E_{bound} \sim \int^{\Lambda} dk \sqrt{M_b^2 + k^2} \sim O(\Lambda^2) + O(\log \Lambda) + \dots \quad (44)$$

When two string are compared it is found that there is a natural way of pairing the states of the two systems. The result of pairing the states is that the quadratic divergence in (44) cancels when two system are compared and the resulting divergence is logarithmic. It is this logarithmic divergences which must be removed by the renormalisation procedure.

These divergences are of exactly the types expected, as standard Feynman diagram calculations in the electroweak theory produce both quadratic and logarithmic divergences. The ultraviolet behaviour of a theory is associated with

very large momentum and thus probes very small distances hence the types of the divergences expected should be independent of any external field configuration.

As discussed in section 3, we are interested in the functional trace,

$$\delta E_{fermion} = -\frac{1}{2} \text{Tr} \left(\sqrt{\hat{H}_1^2} - \sqrt{\hat{H}_2^2} \right), \quad (45)$$

where the two backgrounds being compared have Dirac Hamiltonian operators \hat{H}_1 and \hat{H}_2 . To regulate the divergences we introduce a proper time regulator,

$$\delta E_{fermion}(\tau) = \frac{1}{4\sqrt{\pi}} \int_{\tau}^{\infty} \frac{dt}{t^{\frac{3}{2}}} \text{Tr} (e^{-t\hat{H}_1^2} - e^{-t\hat{H}_2^2}). \quad (46)$$

τ acts as an ultraviolet cut off through the exponential suppression of high momentum contributions and we are interested in the $\tau \rightarrow 0$ limit. It can be seen on dimensional grounds that the proper time regulator, τ , is related to the naive ultraviolet cut off, Λ , by, $\tau \sim \frac{1}{\Lambda^2}$.

We can see that this regulated form reproduces the original trace in the limit $\tau \rightarrow 0$ by using the standard integral [21],

$$\int_{\tau}^{\infty} \frac{dt}{t^{\frac{3}{2}}} e^{-E^2 t} = |E| \Gamma\left(-\frac{1}{2}, E^2 \tau\right) \xrightarrow{\tau \rightarrow 0} \frac{2}{\sqrt{\tau}} - 2\sqrt{\pi} |E| + O(\tau^{\frac{1}{2}}). \quad (47)$$

It is important to note that two systems must be compared so that the $\frac{2}{\sqrt{\tau}}$ term in (47) cancels.

The spectrum of the Dirac Hamiltonian in the background of the Z-string consists of three distinct parts: zero modes, bound states and continuum states, thus the regularised fermionic energy can be written as,

$$E_{fermion}(\tau) = E_{zeromode}(\tau) + E_{boundstate}(\tau) + E_{cont}(\tau),$$

and each of these three parts can be handled separately.

As discussed in section 4, we split the $3+1D$ Dirac Hamiltonian into a $2+1D$ Hamiltonian together with a contribution coming from the momentum of the fermion along length of the string, $\hat{H}_{3+1}^2 = \hat{H}_{2+1}^2 + k_z^2$. The trace must sum over all the allowed values of k_z , remembering that zero modes only move in one direction along the string. We restrict the spinors to a cylindrical box of length L and impose periodic boundary conditions in the z -direction, thus quantising the allowed z -momenta. Taking the limit $L \rightarrow \infty$, the sum over allowed momenta becomes an integral over the momentum parallel to the string in the usual way. As a zero mode only moves in one direction along the string, its contribution is only half that of a massive bound state or a continuum state.

We can now determine the zero mode contribution to the energy per unit length of the string;

$$E_{zeromode}(\tau) = \sum_{zeromodes} \frac{1}{2\sqrt{\pi}} \int_{\tau}^{\infty} \frac{dt}{t^{\frac{3}{2}}} \int_0^{\infty} \frac{dk}{2\pi} e^{-tk^2} = \frac{\alpha_{ZM}}{8\pi} \int_{\tau}^{\infty} \frac{dt}{t^2} = \frac{\alpha_{ZM}}{8\pi} \frac{1}{\tau}, \quad (48)$$

where α_{ZM} denotes the number of zero mode solutions to the $2 + 1D$ Dirac equation. From (48) it can be seen that a zero mode state contributes a purely manifest quadratic divergence to the fermionic energy.

Similarly for a massive bound state solution with effective mass E , the energy contribution per unit length of string is given by,

$$\begin{aligned} E_{boundstate}(\tau) &= \frac{1}{2\sqrt{\pi}} \int_{\tau}^{\infty} \frac{dt}{t^{\frac{3}{2}}} \int_{-\infty}^{\infty} \frac{dk}{2\pi} e^{-tk^2} e^{-tE^2} \\ &= \frac{1}{4\pi} \left(\frac{1}{\tau} + E^2 \log(E^2\tau) + E^2(C - 1) + O(\tau) \right), \end{aligned} \quad (49)$$

where C is Eulers constant. As with the zero modes it can be seen from (50) that each massive bound state contributes a manifest quadratic divergence to the fermionic energy. Moreover in both cases the manifest quadratic divergence is independent of the energy of the state. We shall see in section 8 that these manifest quadratic divergences cancel when two systems are compared as there is a natural way in which to pair states.

Finally the continuum contribution to the fermionic energy per unit length of string reads,

$$E_{cont}(\tau) = \frac{1}{4\pi} \int_{\tau}^{\infty} \frac{dt}{t^2} \text{Tr}_{cont}^+ e^{(-t\hat{H}_{2+1,\lambda}^2)}, \quad (50)$$

where Tr_{cont}^+ denotes a trace over the positive energy part of the continuum spectrum of \hat{H}_{2+1} and we have integrated out the degree of freedom along the direction of the string.

The contributions to $E_{fermion}(\tau)$ from the massive bound states and zero modes are easy to compute once the fermion spectrum is known. The continuum contribution in contrast requires a significant amount of work before it is of a practical form for calculations.

6. Discretising and Recovering the Continuum

In the previous section we determined an expression for the regulated contribution of the continuum to the total fermionic energy in the string background. This involves a trace over the positive energy continuum and consequently introduces a sum over an infinite number of states. To carry out this sum we impose a boundary condition on the spinor profile functions on the surface of a cylinder of radius R_o centred on the core of the string. This condition selects a discrete subset of the continuum states over which we trace. The full continuum is recovered as $R_o \rightarrow \infty$, so the actual trace over the continuum can then be generated by taking this limit. This will be done explicitly so that the discrete sum over the discretised continuum becomes an integral. The use of the discretisation condition is merely an intermediate step in setting up the sum over

the continuum. This step is however critical, because it ensures that the correct density of continuum states is used.

The details of the discretisation procedure are given in appendix A. The boundary condition we impose is that the 1st and 3rd components of the spinors vanish at $r = R_o$.

The Dirac equation in the Z-string background has two regular short distant solutions which match asymptotically onto two linear combinations of the asymptotic solutions given in (40). The boundary conditions lead to a constraint of the form,

$$\frac{J_{|\nu|}(kR_o)}{N_{|\nu|}(kR_o)} = -X(k), \quad (51)$$

where $X(k)$ is given in terms of the matching coefficients.

The left hand side of this constraint is approximately $\cot(kR_o)$ and consists of an infinite number of branches of width proportional to $\frac{1}{R_o}$. The density of the solutions to the discretisation condition thus becomes infinite as $R_o \rightarrow \infty$ and so the full continuum is recovered.

Obtaining a unique solution to the discretisation condition requires careful analysis, principally due to the occurrence of singularities in $X(k)$. This issue is discussed in detail in appendix A.

The discretisation condition can be written uniquely in the form,

$$k_i R_o = k_i^o R_o + \Delta(k_i), \quad (52)$$

where the free momentum is defined by, $k_i^o R_o = i\pi$, and $\Delta(k)$ is determined by matching short distance spinors to asymptotic spinors. The details are given in appendix A.

As, $k_i = k_i^o + O(\frac{1}{R_o})$, we have,

$$k_i R_o = k_i^o R_o + \Delta^\pm(k_i^o) + O(\frac{1}{R_o}). \quad (53)$$

All of the terms on the right hand side depend only on the known free momentum k_i^o . Expanding the momentum in powers of $\frac{1}{R_o}$ we have,

$$e^{-tk_i^2} = e^{-t\left[k_i^o + \frac{1}{R_o}\Delta^\pm(k_i^o) + O(\frac{1}{R_o^2})\right]^2} = e^{-t(k_i^o)^2} \left[1 - t\frac{2k_i^o}{R_o}\Delta^\pm(k_i^o) + O(\frac{1}{R_o^2})\right]. \quad (54)$$

The free momentum k_i^o provides a set of evenly spaced nodes with spacing $\delta k = \frac{\pi}{R_o}$. In the large R_o limit we have,

$$\sum_{i=1}^{\infty} e^{-tk_i^2} = \frac{R_o}{\pi} \int_0^{\infty} dk e^{-tk^2} - \frac{1}{2} - \frac{2t}{\pi} \int_0^{\infty} dk k \Delta^\pm(k) e^{-tk^2} + O(\frac{1}{R_o}). \quad (55)$$

The first term on the right hand side of (55) will be seen to cancel when two systems are compared.

Equation 55 is exactly the integral representation of the continuum contribution to the fermionic energy we require. We have expressed the regularised trace over the continuum states as an integral over the transverse momentum with the integrand defined in terms of matching coefficients found by solving the Dirac equation.

Finally, the total fermionic contribution to the energy of the string from a given angular momentum mode, n , is given by,

$$E_{fermion}^n(\tau) = \frac{\alpha_{ZM}^n}{8\pi} \frac{1}{\tau} + \frac{1}{4\pi} \int_{\tau}^{\infty} \frac{dt}{t^2} \sum_i e^{-tE_{n,i}^2} - \frac{1}{2\pi^2} \int_{\tau}^{\infty} \frac{dt}{t^2} e^{-tg^2} \left[\frac{\pi}{2} - \int_0^{\infty} dk e^{-tk^2} [R_0 - kt \sum_{\pm} \Delta^{\pm,n}(k)] \right] \quad (56)$$

where α_{ZM}^n is the number of zero modes with mode number n , $\{E_{n,i}\}$ is the set of positive energy massive bound state solutions of the $2 + 1D$ Dirac equation and finally $\Delta^{\pm,n}(k)$ are the two functions defined by (152) for the pure Z-string background.

7. Renormalisation Issues

Now we have a regulated expression for the fermionic energy shift we must renormalise it in order to calculate the physical value of the fermionic energy. We focus on the computation of the counter term in the background of the Z-string using the heat kernel expansion. By calculating the counter term required to renormalise the contribution made by each angular momentum mode it is possible to renormalise each mode individually.

The highest order divergence which is expected in the electroweak theory is a quadratic divergence associated with the Higgs mass renormalisation. The remaining divergences are logarithmic in nature, corresponding to the wavefunction renormalisation of the Higgs and gauge fields together with the logarithmic renormalisation of the Higgs self coupling.

The physical energy of the string should be expressed in terms of physical parameters defined at the electroweak scale, rather than the bare parameters that enter the Lagrangian. Consider the sum of the classical string energy and the fermionic energy,

$$E_{string} = E_{classical}^{bare} + E_{fermion}(\tau), \quad (57)$$

where $E_{classical}^{bare}$ is the classical energy per unit length of the string expressed in terms of bare parameters (see (9)) and $E_{fermion}(\tau)$ is the regularised fermionic energy. The divergences arising in the fermionic energy should be combined with the classical energy defined in terms of the bare parameters to give an expression for the classical energy defined in terms of the physical parameters defined at some scale μ .

In the proper time regularisation scheme we have,

$$E_{fermion}(\tau) = \frac{1}{8\pi} \int_{\tau}^{\infty} \frac{dt}{t^2} \text{Tr} e^{-t\hat{H}^2}.$$

The integral over the proper time t can be split into two pieces, $\tau \rightarrow \mu$ and $\mu \rightarrow \infty$, where μ is some arbitrary scale (eventually μ will be set equal to M_Z^{-2}). We use the heat kernel expansion to isolate the divergent contributions arising in the small τ limit of the first integral above and determine the counter term,

$$E_{CT}(\tau, \mu) = \frac{1}{8\pi} \int_{\tau}^{\mu} \frac{dt}{t^2} \text{Tr} e^{-t\hat{H}^2} |_{div.} . \quad (58)$$

Consistency of the renormalisation scheme requires that no physical quantity depends on the scale μ . This will be ensured by renormalisation group invariance, provided the terms which comprise $E_{CT}(\tau, \mu)$ take the same form as those which arise in $E_{classical}^{bare}$ and there exist unique expressions relating the bare parameters to the renormalised parameters. These conditions are satisfied in the electroweak theory when the proper time regulator is used [24]. E_{string} is thus invariant under changes in μ and so the value of μ will be set to an energy scale characteristic of the electroweak theory and the parameters of the theory set to their values at this energy scale. Specifically, $\mu = M_Z^{-2}$.

In the electroweak theory anomalies cancel between the quark and lepton sectors. As we consider only quarks, there is the possibility of anomalous divergences appearing that can only be cancelled by including leptons. However, as the two systems being compared are in the same topological sector, no anomalous divergences arise.

To compute the counter term we use the heat kernel method. First we review the method and then we apply it in the string background.

Consider an operator, \hat{O} , and the associated heat equation,

$$\frac{\partial}{\partial t} H(t; x, y) + \hat{O}_x H(t; x, y) = 0. \quad (59)$$

The trace of interest is then given by [22],

$$\text{Tr} e^{-t\hat{O}} = \text{Tr} \int d^d x H(t; x, y). \quad (60)$$

It is important to make the distinction between the two types of traces which appear in (60), the trace on the left hand side is a functional trace over a complete set of states whereas the trace on the right hand side is a standard matrix trace.

It is well known that the heat equation possess an asymptotic solution in terms of the heat kernel expansion defined by [22, 23],

$$H(t; x, y) = \frac{1}{(4\pi t)^{\frac{d}{2}}} \exp\left(\frac{|x-y|^2}{4t}\right) \sum_{n=0}^{\infty} a_n(x, y) t^n. \quad (61)$$

(61) is a power series expansion for small proper time t . The functions $a_n(x, y)$ are the heat kernel expansion coefficients, their precise form will be derived later. Substitution of (61) into (60) implies that,

$$\text{Tr } e^{-t\hat{O}} = \frac{1}{(4\pi t)^{\frac{d}{2}}} \sum_{n=0}^{\infty} t^n \int d^d x \text{Tr } [a_n] \quad (62)$$

where $[a_n] = a_n(x, x)$.

By direct substitution of (61) into (59) and equating powers of t it is straightforward to derive a recurrence relation for the coefficients a_n .

The counter term defined at some subtraction point, μ , involves a trace over the $2 + 1D$ Dirac Hamiltonian defined in the plane perpendicular to the string. Therefore $d = 2$ in the heat kernel expansion and we have,

$$E_{CT}(\tau; \mu) = \frac{1}{32\pi^2} \int d^2 x \left(\frac{1}{2} \left(\frac{1}{\tau^2} - \frac{1}{\mu^2} \right) \text{Tr}[a_0] + \left(\frac{1}{\tau} - \frac{1}{\mu} \right) \text{Tr}[a_1] + \log\left(\frac{\mu}{\tau}\right) \text{Tr}[a_2] \right), \quad (63)$$

where we have kept only the divergent terms. It is clear from (63) that the $[a_1]$ term corresponds to the quadratic counter term and the $[a_2]$ term correspond to the logarithmic counter term. The quartic divergence arising from the $[a_0]$ term cancels when two systems are compared.

To derive the counter term only the coefficients $[a_1]$ and $[a_2]$ need to be calculated. They are found to be,

$$\text{Tr } [a_1] = -4g^2 f(r)^2, \quad (64)$$

$$\begin{aligned} \text{Tr } [a_2] = & \frac{2}{3} (\alpha_L^2 + \alpha_R^2) \left(\frac{\nu(r)'}{r} \right)^2 + 2g^4 f(r)^4 + 2g^2 \left((f(r)')^2 + \left(\frac{f(r)}{r} \right)^2 \right) \\ & + 4g^2 \frac{\nu(r) f(r)^2}{r^2} + 2g^2 \frac{\nu(r)^2 f(r)^2}{r^2}, \end{aligned} \quad (65)$$

where $f(r)$ and $\nu(r)$ are the Higgs and gauge field profiles of the string respectively.

In this section the forms of both the quadratic and logarithmic counter terms have been derived using the heat kernel expansion. The next step is to calculate the difference between the fermionic energies of two strings. In the next section such a calculation is carried out using a toy model which provides significant insight into the calculation of fermionic energies.

8. The Core Model

Before attempting a full numerical calculation of the fermionic energy in the Z-string background, it is very instructive to consider a more analytical treatment in a simplified model. To this end we use a core model in which simplified profiles replace the actual Nielsen Olesen profiles. Exact expressions for the spinor wavefunctions can then be written down, the discretisation condition can be constructed analytically and insight into some of its important properties can be gained.

8.1 The Model

We use a core model defined by replacing the Nielsen-Olesen profile functions by,

$$f(r) = \nu(r) = \theta(r - R_c), \quad (66)$$

where $\theta(x)$ is the Heaviside step function. Clearly these profiles do not satisfy the Nielsen-Olesen equations, however it is still a perfectly valid exercise to investigate fermions in this background. The behaviour of the core model profiles for $r > R_c$ is identical to the asymptotic behaviour of the Nielsen-Olesen profiles, particles will therefore have their usual vacuum masses for $r > R_c$. While for $r < R_c$, both the Higgs and gauge fields vanish and all particles are massless.

The scattering of fermions off the core model string has been investigated in [25] and [26], for completeness some of their results will be rederived.

8.2 Core Model Spinors

To find the global solutions of the Dirac equation we solve the Dirac equations in the regions $r < R_c$ (internal) and $r > R_c$ (external) then impose continuity of the spinors at $r = R_c$. For $r > R_c$ the general continuum ($E^2 > g^2$) solution is given by (40) with, $\nu = n - \lambda + \alpha_L$. We now drop the subscript λ in the definition of ν for clarity. Similarly, the general external bound state solution ($E^2 < g^2$) is given by (41).

The general regular internal solution reads,

$$\Psi_{r < R_c} = \alpha \begin{pmatrix} J_n(Er) \\ -J_{n+1}(Er) \\ 0 \\ 0 \end{pmatrix} + \beta \begin{pmatrix} 0 \\ 0 \\ J_{n-\lambda}(Er) \\ J_{n-\lambda+1}(Er) \end{pmatrix}. \quad (67)$$

For $r < R_c$ the fermions are massless, the mass-shell condition reads $E^2 = k^2$ and the argument of these solutions is Er . These solutions are therefore suitable for use in the bound state energy region as well as the continuum regions.

The spinor profiles must be continuous at $r = R_c$. For continuum states this gives matching conditions which allow us to determine the scattering coefficients analytically.

In the case of bound states we only have two regular asymptotic spinors and the system of constraints is over specified. Non-trivial solutions to the matching conditions are then possible if and only if,

$$\begin{vmatrix} EK_{\nu+1}(kR_c)J_n(ER_c)+ & gK_{\nu+1}(kR_c)J_n(ER_c) \\ kK_{\nu}(kR_c)J_{n+1}(ER_c) & \\ gK_{\nu+1}(kR_c)J_{n-\lambda}(ER_c) & EK_{\nu+1}(kR_c)J_{n-\lambda}(ER_c)+ \\ & kK_{\nu}(kR_c)J_{n-\lambda+1}(ER_c) \end{vmatrix} = 0. \quad (68)$$

This condition clearly puts restrictions on the energy values for which physical bound state wavefunctions exist and so generates a discrete bound state spectrum.

Just as in the case of the actual Z-string there are also zero mode solutions. These occur in the $n = 0$ mode for the up quark and in the $n = -1$ mode for the down quark. The internal solutions in the zero mode case are simply constants, while the external solutions decay exponentially at large r .

8.3 Core Model Discretisation, State Pairing and Spectral Flow

In appendix A we discuss in detail how to discretise the continuum by imposing boundary conditions on the spinor profiles at some large radial distance, $r = R_o$. The advantage of the core model is that analytic expressions are known for the scattering coefficients and so an analytic expression can be written down for the discretisation condition.

Each spinor in the discretised continuum consists of a linear combination of the two regular internal solutions. We denote the relative amount of each regular internal solution in the spinor by γ . In deriving the discretisation condition we obtain a quadratic equation for γ (147). By direct substitution of the scattering coefficients into (148), (149) and (150) we find explicit forms for the coefficients and the quadratic reduces to,

$$\gamma^2(gJ_{n+1}J_n) + \gamma E(J_{n+1}J_{n-\lambda} - J_nJ_{n-\lambda+1}) - gJ_{n-\lambda+1}J_{n-\lambda} = 0. \quad (69)$$

We have solutions,

$$\gamma = \frac{-E(J_{n+1}J_{n-\lambda} - J_nJ_{n-\lambda+1}) \pm \sqrt{\Delta}}{2gJ_nJ_{n+1}} \quad (70)$$

where the discriminant, Δ , is given by,

$$\Delta = E^2(J_{n+1}J_{n-\lambda} - J_nJ_{n-\lambda+1})^2 + 4g^2J_nJ_{n+1}J_{n-\lambda+1}J_{n-\lambda}. \quad (71)$$

The argument of all the Bessel functions in (69)-(71) is ER_c . There are four cases to be considered, corresponding to $|\nu| = \pm\nu$ and to the two roots of the quadratic equation. Explicitly the discretisation condition becomes,

$$\frac{J_{|\nu|}(kR_o)}{N_{|\nu|}(kR_o)} = X_{\zeta|\nu|}^{\pm} \quad \text{for } |\nu| = \zeta\nu \quad (72)$$

where,

$$X_{\zeta|\nu|}^{\pm} = \frac{E(J_{n+1}J_{n-\lambda} + J_{n-\lambda+1}J_n)J_{|\nu|} \mp J_{|\nu|}\sqrt{\Delta} - 2\zeta k J_n J_{n-\lambda} J_{|\nu|+1}}{E(J_{n+1}J_{n-\lambda} + J_{n-\lambda+1}J_n)N_{|\nu|} \mp N_{|\nu|}\sqrt{\Delta} - 2\zeta k J_n J_{n-\lambda} N_{|\nu|+1}} \quad (73)$$

Throughout, unless the argument is explicitly given, the Bessel functions of integral order, associated with internal solutions, have argument ER_c , whereas those of orders involving $|\nu|$ have argument kR_c .

Using the small argument expansions of the Bessel functions it is fairly straightforward to show that,

$$\begin{aligned} X_{|\nu|}^{\pm}(k) &\stackrel{k \rightarrow 0}{\sim} 0 && \nu > 0 \\ X_{-|\nu|}^{+}(k) &\stackrel{k \rightarrow 0}{\sim} \tan(|\nu| \pi) && -1 < \nu < 0 \\ X_{-|\nu|}^{-}(k) &\stackrel{k \rightarrow 0}{\sim} 0 && -1 < \nu < 0 \\ X_{-|\nu|}^{\pm}(k) &\stackrel{k \rightarrow 0}{\sim} 0 && \nu < -1. \end{aligned}$$

Similarly, using large argument expansions of the Bessel functions we find as $k \rightarrow \infty$,

$$X_{|\nu|}^{+} \sim \cot \frac{\pi}{2}(n - |\nu|), \quad X_{|\nu|}^{-} \sim \cot \frac{\pi}{2}(n - |\nu| - \lambda), \quad (74)$$

$$X_{-|\nu|}^{+} \sim -\cot \frac{\pi}{2}(|\nu| - n), \quad X_{-|\nu|}^{-} \sim -\cot \frac{\pi}{2}(|\nu| - n - \lambda). \quad (75)$$

It is important to note that the infinite momentum behaviour of these functions is independent of the core radius R_c .

We can now calculate the fermionic energy difference between two core model strings with different core radii. This model calculation will illustrate many of the features of the full calculation, but in a more manageable context.

The eigenvalues are expected to be continuous functions of the core radius, R_c . As a result a 1 : 1 correspondence should exist between the fermionic eigenvalues of the two strings. We first verify this by analysing a specific example. This provides insight into the physical interpretation of the singularity structure of the functions $X^{\pm}(k)$.

As the core radius, R_c , is varied a continuous flow of the energy eigenvalues is expected, with the total number of fermionic states remaining constant. If a continuum state close to threshold loses energy and falls into the bound state region, a new bound state solution appears. Consequently, one of the infinitely many continuum states has become a bound state. It is essential when comparing two systems that the correct number of states are counted in each system so that the total number counted is the same in both cases, failure to do so would result in the occurrence of divergences which are not removed by the counter term.

For finite R_o the solutions of the discretisation condition are the points where the graph of $\frac{J_{|\nu|}(kR_o)}{N_{|\nu|}(kR_o)}$ intercepts the graphs of $X_{\pm|\nu|}^{\pm}$. The function $\frac{J_{|\nu|}(kR_o)}{N_{|\nu|}(kR_o)}$ behaves

like $\cot(kR_o - \frac{|\nu|\pi}{2} - \frac{\pi}{4})$ for $kR_o \gg 1$, so there are an infinite number of branches with a width proportional to $\frac{1}{R_o}$. The singularities and zeros of $\frac{J_{|\nu|}(kR_o)}{N_{|\nu|}(kR_o)}$ clearly occur at the zeros of $N_{|\nu|}(kR_o)$ and $J_{|\nu|}(kR_o)$ respectively.

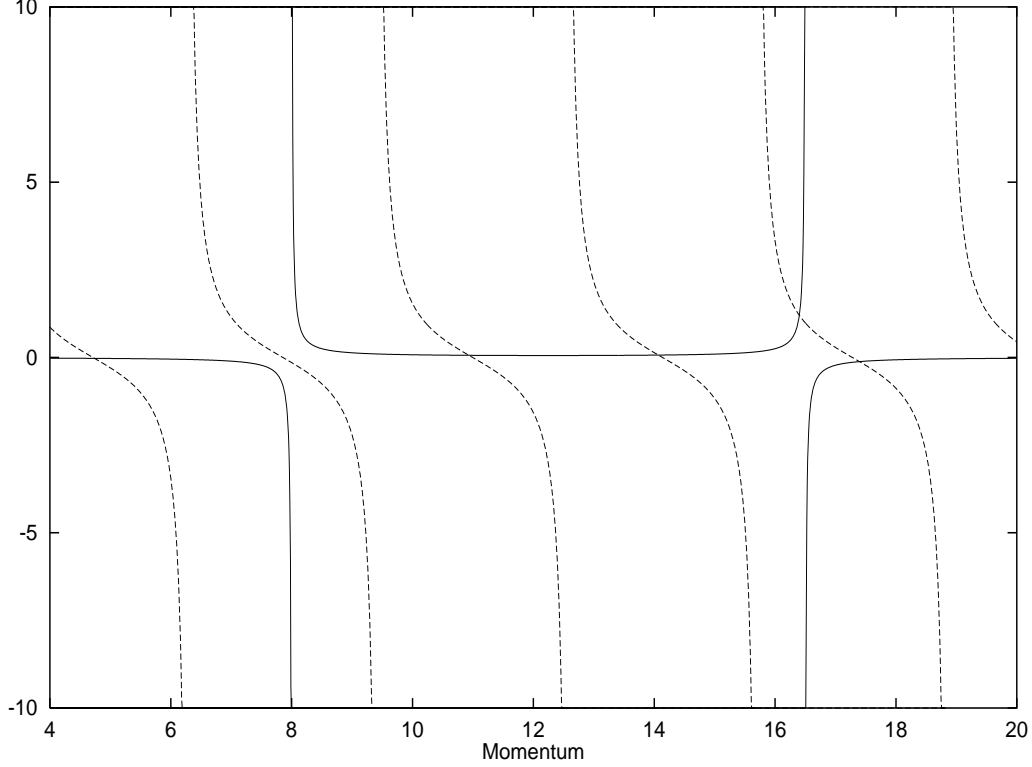


Figure 1: Singularities in $X^\pm(k)$ and extra/missing states. The solid line shows a Type 1 and a Type 2 singularity in $X^\pm(k)$ respectively. States are found at the intersections of this line and the dashed line.

The non-zero roots of $J_{|\nu|}(kR_o)$ act as a suitable set with which the solutions of the discretisation condition (72) can be matched, and thus provide a means of counting the continuum states. Complications arise, as discussed in appendix A, due to the singularities in $X^\pm(k)$. For each Type 1 singularity there is one zero of $J_{|\nu|}(kR_o)$ for which there is no solution of the discretisation condition [fig.1]. Conversely, for each Type 2 singularity there is one zero of $J_{|\nu|}(kR_o)$ for which there are two solutions of the discretisation condition. The number of states will be denoted by $(1 : 1)_{|\nu|} - q$, where the notation signifies that each solution of the discretisation condition can be paired with a non-zero root of $J_{|\nu|}(kR_o)$ with q non-zero roots of $J_{|\nu|}(kR_o)$ being left unpaired.

This process is independent of the specific value of R_o . As R_o is increased the

density of branches of $\frac{J_{|\nu|}(kR_o)}{N_{|\nu|}(kR_o)}$ increases but the resulting state count does not change, because the functions $X_{\pm|\nu|}^{\pm}(k)$ are independent of R_o .

To illustrate this we consider two core model strings, one with $R_c = 0.5$ and the other with $R_c = 1$. The parameters used are, $\theta_w = 0.5, g = 1.0$. Summing over the \pm solutions for modes $n = -2..2$ for both core radii, we find $2(1 : 1)_{|\nu|}$ states in all cases except for the function $X^+(k)$ in the $n = -1$ mode. This difference arises because of the existence of a Type 1 singularity for $R_c = 1.0$ in $X^+(k)$ [fig.2]. This leaves one non-zero root of the appropriate Bessel function $J_{|\nu|}(kR_o)$ unpaired in the counting process.

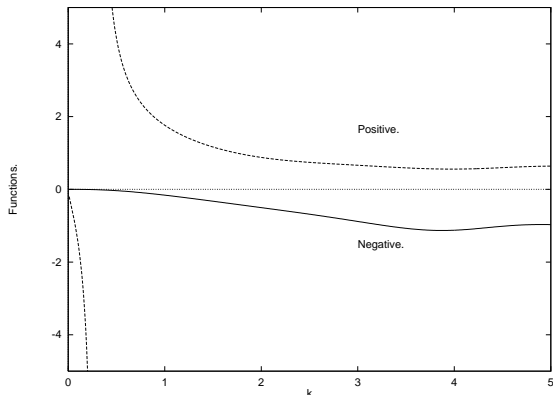


Figure 2: $X^{\pm}(k)$ for the up quark with $n = -1$ and $R_c = 1$.

To find the total number of states we must also include any massive bound states and zero modes. For $R_c = 1.0$ there is just one massive up quark bound state and it resides in the $n = -1$ mode. No massive up quark bound states exist for $R_c = 0.5$. Thus spectral flow has taken a continuum state and produced a bound state.

The inclusion of the zero modes is more subtle as they only move in one direction along the string. A zero mode should only contribute $\frac{1}{2}$ to the state count of the mode in which it arises. In the $2 + 1D$ context the zero mode should therefore count as only half a state. This is an example of fermion number fractionization [27, 28], but it has been motivated by looking at the full $3 + 1D$ system.

As expected, the total state count is the same within each mode hence the total number of string states is the same. It is worth noting that the state counting matches within each mode because there is no spectral flow between different angular momentum sectors as the core radius, R_c , is varied.

The state counting procedure can be repeated using exactly the same techniques for the down quark. Again we find the same total state count in both backgrounds.

Having verified that the total number of fermionic states within a given mode does not change as R_c varies, we attempt to compute the fermionic energy difference of the two core model strings.

8.4 The Core Model Fermionic Energy Shift

Using (56), the difference in fermionic energy within a given mode for two systems denoted 1 and 2 is,

$$\begin{aligned} \Delta E^n(\tau) &= \frac{(\alpha_{1,zm}^n - \alpha_{2,zm}^n) \frac{1}{\tau}}{8\pi} + \frac{1}{4\pi} \int_{\tau}^{\infty} \frac{dt}{t^2} \left(\sum_{i_1} e^{-tE_{n,i_1}^2} - \sum_{i_2} e^{-tE_{n,i_2}^2} \right) \\ &\quad - \frac{1}{2\pi^2} \int_{\tau}^{\infty} \frac{dt}{t} e^{-tg^2} \int_0^{\infty} dk k e^{-tk^2} \sum_{\pm} \left(\Delta_1^{\pm,n}(k) - \Delta_2^{\pm,n}(k) \right), \end{aligned}$$

where the continuum contribution is encapsulated in the functions $\Delta(k)$ defined by,

$$\Delta(k) = \beta_{\infty} \pi + \theta_{\nu} + \cot^{-1}(X(k)) \Big|_p^{\text{cont}}.$$

The θ_{ν} terms cancel and the continuum contribution becomes,

$$- \frac{1}{4\pi} \int_{\tau}^{\infty} \frac{dt}{t} e^{-tg^2} \sum_{\pm} \left[(\beta_{1,\infty}^{\pm} - \beta_{2,\infty}^{\pm}) + \frac{2}{\pi} \int_0^{\infty} dk k e^{-tk^2} \begin{pmatrix} \cot^{-1}(X_1^{\pm}(k)) \Big|_p^{\text{cont}} \\ - \cot^{-1}(X_1^{\pm}(k)) \Big|_p^{\text{cont}} \end{pmatrix} \right]. \quad (76)$$

In the core model the large momentum limit of the functions $X(k)$ is a constant which is independent of the core radius. Thus the $\cot^{-1}(X_1^{\pm}(k)) \Big|_p^{\text{cont}} - \cot^{-1}(X_1^{\pm}(k)) \Big|_p^{\text{cont}}$ term tends to zero for large momentum.

As discussed in appendix A, the coefficients of the first integral in (77) can be deduced by simply counting the singularities of the functions $X^{\pm}(k)$,

$$\beta_{1,\infty}^{\pm} - \beta_{2,\infty}^{\pm} = \left(\begin{array}{c} \text{No. Type 1 of } X_1^{\pm} \\ - \text{No. Type 1 of } X_2^{\pm} \end{array} \right) - \left(\begin{array}{c} \text{No. Type 2 of } X_1^{\pm} \\ - \text{No. Type 2 of } X_2^{\pm} \end{array} \right). \quad (77)$$

For the up quark, the only singularity in the functions $X^{\pm}(k)$ occurs for the + sign case in the $n = -1$ mode. Thus we have, $\beta_{1,\infty}^{\pm} - \beta_{2,\infty}^{\pm} = 0$, in all cases except for the + sign case in the $n = -1$ mode, where the type 1 singularity in $X_1^{+,n=-1}(k)$ implies that $\beta_{1,\infty}^+ - \beta_{2,\infty}^+ = 1$.

In all case except for the + sign case in the $n = -1$ mode, the energy difference for each solution within a given mode reads,

$$\Delta E_{\pm}^n(\tau) = - \frac{1}{2\pi^2} \int_{\tau}^{\infty} \frac{dt}{t} e^{-tg^2} \int_0^{\infty} dk k e^{-tk^2} \left(F^{\pm,n}(k) \right), \quad (78)$$

where,

$$F^{\pm,n}(k) = \left(\cot^{-1}(X_1^{\pm,n}(k) \Big|_p) - \cot^{-1}(X_2^{\pm,n}(k) \Big|_p) \right). \quad (79)$$

In the special case [+ sign, $n = -1$] we have,

$$\Delta E_+^{n=-1}(\tau) = \frac{1}{4\pi} \int_{\tau}^{\infty} \frac{dt}{t^2} \left[e^{-tE_{n=-1,1}^2} - e^{-tg^2} \left[1 - \frac{2t}{\pi} \int_0^{\infty} dk k F^{+,-1}(k) \right] \right]. \quad (80)$$

The first term in (80) is the standard bound state contribution due to the existence of the massive bound state in this mode when $R_c = 1.0$. The second term is more subtle, it is due to the Type 1 singularity in $X^{+,-1}(k)$ which gives, for this particular case, $\beta_{1,\infty}^{+,-1} - \beta_{2,\infty}^{+,-1} = 1$ and introduces an extra term from (76). This term looks exactly like a massive bound state contribution except the state has threshold energy and the term arises with an overall minus sign relative to the massive bound state. In the state counting the Type 1 singularity in $X^{+,-1}(k)$ ensured that there are the same number of states in each mode for both string backgrounds. Spectral flow considerations suggest that the natural state to pair up with a massive bound state is a continuum state with threshold energy. Such a state would make exactly this contribution to the fermionic energy. These observations show that our formulation of the discretisation condition produces the desired state counting and matches states up in a consistent manner.

Whilst an individual bound state contributes a manifest quadratic divergence, the coefficient of this divergence is independent of the energy of the state. Thus this pairing of a massive bound state with a threshold state cancels the quadratic divergences. This is to be expected from our naive arguments using a momentum cut-off: while the total fermionic energy must be quadratically divergent, the bound states only move along the direction of the string and so they only contribute a logarithmic divergence.

The total continuum contribution made by a particular mode is determined by the sum $F^{+,n}$ and $F^{-,n}$,

$$F^n(k) = \sum_{\pm} F^{\pm,n}(k). \quad (81)$$

For all modes the function $F^n(k)$ tends to zero at large k , while at small k we find $F^n(0) = 0$ for all modes except for the $n = -1$ mode, where $F^{-1}(0) = -\pi$ (fig.3). This is an example of Levinson's Theorem [29] which relates the number of bound states to the associated phase shift. In the notation used here, Levinson's Theorem states that the number of massive bound states of the first string minus the number of massive bound states of the second string is equal to $-\frac{F(0)}{\pi}$.

We should now subtract the counter terms to obtain a finite energy difference. The quadratic counter term can then be compared to the behaviour of the fermionic energy as τ tends towards zero and the quadratic renormalisation can be implemented. However there is a pathology with the logarithmic counter term which prevents a full renormalisation of the core model. We can however demonstrate several important features of the calculation, in particular the convergence with mode number.

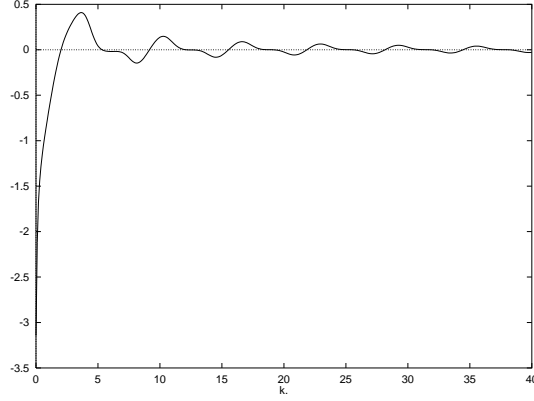


Figure 3: $F^{-1}(k)$ for the up quark with $\theta_w = 0.5$, $g = 1.0$, $R_{c,1} = 1.0$ and $R_{c,2} = 0.5$.

Using (63), the divergent part of the quadratic counter term is,

$$E_{Quad}(\tau) |_{Div} = \frac{1}{16\pi} \frac{1}{\tau} \int_0^\infty dr r \text{Tr} \Delta[a_1] = -\frac{g^2}{4\pi} \frac{1}{\tau} \int_0^\infty dr r (f_1(r)^2 - f_2(r)^2), \quad (82)$$

where the subscripts refer to strings 1 and 2. Using the definition of the core model profile functions (66), we have,

$$E_{Quad}(\tau) |_{Div} = \frac{g^2}{8\pi} \frac{1}{\tau} [R_{c1}^2 - R_{c2}^2] = \frac{3g^2}{32\pi} \frac{1}{\tau}, \quad (83)$$

for the example considered ($R_{c1} = 1.0$, $R_{c2} = 0.5$).

The coefficient of $\frac{1}{\tau}$ in (83) should be compared with,

$$\lim_{\tau \rightarrow 0} \tau \sum_{n=-\infty}^{\infty} \Delta E^n(\tau), \quad (84)$$

where $\Delta E^n(\tau)$ is defined by (78) and (80). The convergence of the sum over n is of critical importance both fundamentally and practically. Each $\Delta E^n(\tau)$ must be calculated numerically and hence in practice the sum must be computed up to some finite value of n , n_{max} , and at some finite value of τ . We will demonstrate that for a given value of τ , providing the value of n_{max} is sufficiently large, the higher terms in the sum over n are indeed small and convergence is ensured.

The reason for this convergence can be seen by looking at the form of the energy shift functions, $F^n(k)$. Figure 4 shows the functions $F^n(k)$ as a function of k for $n = 5, 10, 15$ for the up quark, the features are however generic. As n increases, the functions $F^n(k)$ remain close to zero for a larger range of k before the oscillations begin. This is due to the spinor profiles. They are Bessel functions

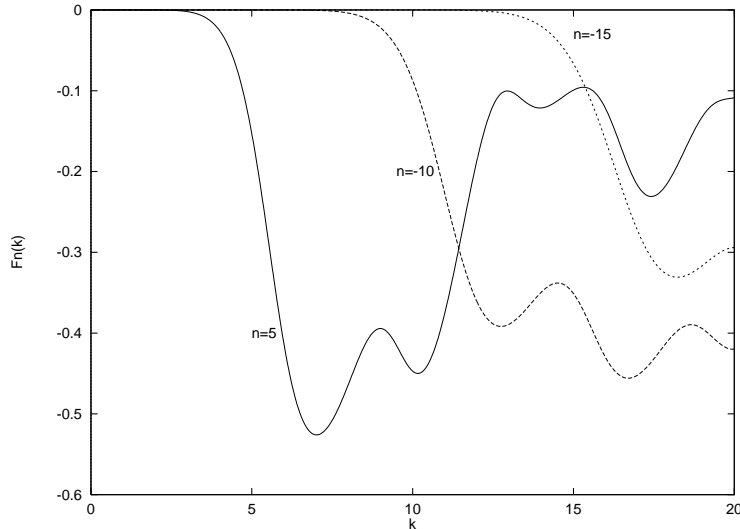


Figure 4: The functions $F^n(k)$ for the up quark with $n = 5, 10, 15$.

and so power law suppressed until their argument is of the same magnitude as their order [21].

The proper time regulator introduces the exponential suppression factor e^{-tk^2} into the energy integral. As the absolute value of the mode number increases, the region where the functions $F^n(k)$ are small (ie. $k < n$) becomes larger and there is increased suppression of the overall contribution. Thus overall we expect a suppression of the form, $e^{-\tau n^2}$.

Physically the modes with high angular momentum do not penetrate the core of the string and as a result are not affected much by changes within the string core.

The total fermionic contribution made by a given angular momentum mode is found by computing the momentum integrals (78) and (80) and summing over the two cases which arise for each mode. The fermionic energy is found to decrease as the absolute value of the mode number n increases, but more slowly as the cut-off τ becomes smaller.

From a numerical point of view the momentum integral must also be truncated at some finite value. This value must be sufficiently large so that the exponential suppression has taken effect. As the value of the cut-off τ is taken to zero, the values of both k and n at which the exponential suppression takes effect become larger, consequently we must extend the range of integration in k and include more modes in order for the sum over n to converge. For the purposes of numerical calculation, if the momentum integrand is required to be suppressed by a factor tol from order unity at the truncation point, the minimum value of

momentum at which the integral can be cut-off is given by,

$$k_{min} \sim \sqrt{\frac{\log tol}{-\tau}}. \quad (85)$$

The maximum mode number used should be of the same order as k_{min} to ensure that the contributions made by higher n modes are also negligible.

It is now possible to compare the coefficients of the quadratic divergence and the quadratic counter term. Figure 5 shows a plot of the total regularised fermionic energy multiplied by the cut-off τ as a function of τ . The 400 lowest angular momentum modes were included in the sum. The horizontal line is the coefficient of the quadratic counter term which has the value 0.02984 for the parameters used.

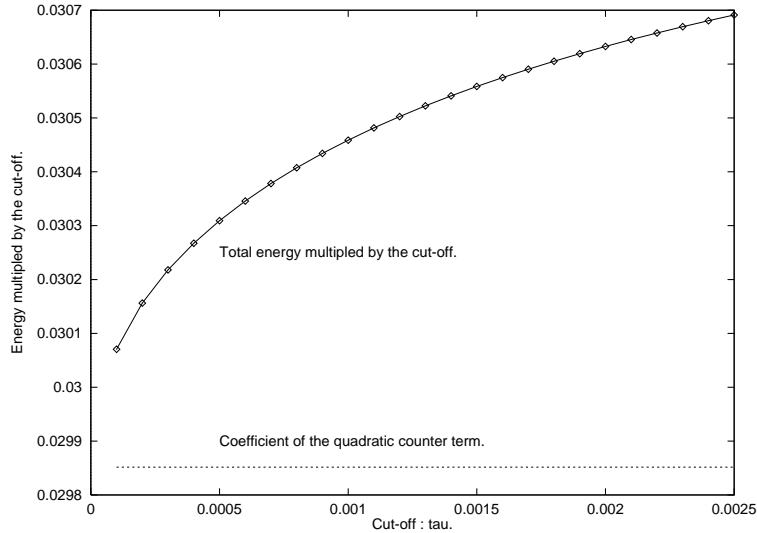


Figure 5: The total regularised fermionic energy multiplied by the cut-off.

It can be seen from figure 5 that $\tau E(\tau)_{fermion}$ is tending towards the coefficient of the quadratic counter term, shown by the horizontal line. Thus we have control of the quadratic divergences. The curvature in $\tau E(\tau)_{fermion}$ becomes more significant as τ becomes small due to the effects of the logarithmic divergence.

Unfortunately we cannot implement logarithmic renormalisation in the core model. The problem arises because the discontinuous nature of the core model profile functions implies that the energy per unit length of the string is infinite. The Higgs field gradient term, for example, gives a contribution,

$$\int_0^\infty dr r (f'(r))^2 = \int_0^\infty dr r \delta^2(r - R_c), \quad (86)$$

which is divergent.

Gradient terms of an identical form arise in the expression for the logarithmic counter term (65), giving rise to the wavefunction renormalisation of both the Higgs and gauge fields. As a result the logarithmic counter term is not defined in the core model background and so logarithmic renormalisation cannot be carried out.

The core model has provided useful insights into the problem and tested critical aspects of our formalism. It has provided insight into the process of counting the fermionic states in the string background, in particular we have demonstrated that the total number of fermionic states is the same for two string configurations with different profile functions. The physical significance of the singularities in the functions $X^\pm(k)$ has been demonstrated: a Type 1 singularity corresponds to the occurrence of a massive bound state. The technology of fixing the discretisation condition uniquely has been shown to ensure that the correct number of states are included in the energy sum. In particular, we have seen that a massive bound state becomes naturally paired with a state at the bottom of the continuum, in accord with spectral flow considerations. An example of Levinson's theorem has been observed, with $-\frac{F(0)}{\pi}$ being the difference in the number of massive bound states in the two systems. Finally, the core model has demonstrated how the convergence of the sum over angular momentum modes arises. This convergence is critical for the success of the method, as numerical computations only ever allow a finite number of modes to be considered.

9. The Perturbed String

We now turn to the calculation of the fermionic energy difference between an actual Z-string and a perturbed Z-string. This will tell us what effect a perturbation in the fields that cause the Z-string to be non-topological has on the fermionic energy. The perturbations we shall consider involve the upper component of the Higgs field becoming non-zero. We set $\phi_+ = g(r)$, where $g(r)$ is some radial profile function which vanishes as $r \rightarrow \infty$.

9.1 The Perturbed String Dirac Equation

The upper component of the Higgs field couples the up and down quarks, hence the Dirac equation will have 8 components. Explicitly the $(2+1)D$ time independent Dirac equation reads,

$$E \begin{pmatrix} u_R \\ u_L \\ d_R \\ d_L \end{pmatrix} = \begin{pmatrix} -i\sigma^i D_i^{u,R} & -g_u \phi_o & 0 & g_u \phi_+ \\ -g_u \phi_o^* & i\sigma^i D_i^{u,L} & -g_d \phi_+ & 0 \\ 0 & -g_d \phi_+^* & -i\sigma^i D_i^{d,R} & -g_d \phi_o^* \\ g_u \phi_+^* & 0 & -g_d \phi_o & i\sigma^i D_i^{d,L} \end{pmatrix} \begin{pmatrix} u_R \\ u_L \\ d_R \\ d_L \end{pmatrix}, \quad (87)$$

where all the covariant derivatives are defined in the background of the unperturbed Z-string and each of the spinors u_R, u_L, d_R, d_L has two components.

Using the standard Z-string ansatz and $\phi_+ = g(r)$ together with the mode decomposition,

$$\begin{pmatrix} u_R \\ u_L \\ d_R \\ d_L \end{pmatrix} = \sum_{n=-\infty}^{\infty} \begin{pmatrix} u_1^R(r)e^{i(n+1)\theta} \\ -iu_2^R(r)e^{i(n+2)\theta} \\ u_1^L(r)e^{in\theta} \\ -iu_2^L(r)e^{i(n+1)\theta} \\ d_1^R(r)e^{in\theta} \\ -id_2^R(r)e^{i(n+1)\theta} \\ d_1^L(r)e^{i(n+1)\theta} \\ -id_2^L(r)e^{i(n+2)\theta} \end{pmatrix} \quad (88)$$

we find the following set of 8 first order, ordinary differential equations for the radial spinor profile functions,

$$Eu_1^R = \left(-\partial_r - \frac{(n+2)}{r} + \alpha_R^u \frac{\nu(r)}{r}\right)u_2^R - g_u f(r)u_1^L + g_u g(r)d_1^L, \quad (89)$$

$$Eu_2^R = \left(\partial_r - \frac{(n+1)}{r} + \alpha_R^u \frac{\nu(r)}{r}\right)u_1^R - g_u f(r)u_2^L + g_u g(r)d_2^L, \quad (90)$$

$$Eu_1^L = \left(\partial_r + \frac{(n+1)}{r} + \alpha_L^u \frac{\nu(r)}{r}\right)u_2^L - g_u f(r)u_1^R - g_d g(r)d_1^R, \quad (91)$$

$$Eu_2^L = \left(-\partial_r + \frac{n}{r} + \alpha_L^u \frac{\nu(r)}{r}\right)u_1^L - g_u f(r)u_2^R - g_d g(r)d_2^R, \quad (92)$$

$$Ed_1^R = \left(-\partial_r - \frac{(n+1)}{r} + \alpha_R^d \frac{\nu(r)}{r}\right)d_2^R - g_d f(r)d_1^L - g_d g(r)u_1^L, \quad (93)$$

$$Ed_2^R = \left(\partial_r - \frac{n}{r} + \alpha_R^d \frac{\nu(r)}{r}\right)d_1^R - g_d f(r)d_2^L - g_d g(r)u_2^L, \quad (94)$$

$$Ed_1^L = \left(\partial_r + \frac{(n+2)}{r} + \alpha_L^d \frac{\nu(r)}{r}\right)d_2^L - g_d f(r)d_1^R + g_u g(r)u_1^R, \quad (95)$$

$$Ed_2^L = \left(-\partial_r + \frac{(n+1)}{r} + \alpha_L^d \frac{\nu(r)}{r}\right)d_1^L - g_d f(r)d_2^R + g_u g(r)u_2^R. \quad (96)$$

This set of equations can easily be seen to decouple into the profile equations for the up and down quark in the background of the pure Z-string, (30) to (33), if $g(r) = 0$. As $g(r)$ vanishes at large radial distances, the system decouples asymptotically into 2 systems, one for the up quark and one for the down quark. Thus the asymptotic solutions are given by (40) and (41) for continuum and bound states respectively.

It is important to note that the orthogonal subspace spanned by spinors with mode number n in (88) is also spanned by unperturbed up quark spinors with mode number $(n+1)$ and the down quark spinors with mode number n as defined by the mode decomposition (29).

9.2 Perturbed String Discretisation

Of the 8 solutions of the Dirac profile equations (89) to (96), 4 are regular at short distance. A spinor describing a physical state must consist of a linear combination of these 4 regular short distance spinors and will match onto a unique linear combination of the 8 regular large distance solutions. Denoting the regular short distance spinors by \vec{S}_i where $i = 1, 2, 3, 4$, we have,

$$\alpha_1 \vec{S}_1 + \alpha_2 \vec{S}_2 + \alpha_3 \vec{S}_3 + \alpha_4 \vec{S}_4 \rightarrow \begin{pmatrix} M_u & 0 \\ 0 & M_d \end{pmatrix} \begin{pmatrix} \vec{a}_u \\ \vec{a}_d \end{pmatrix}, \quad (97)$$

where $\vec{a}_{u,d}^T = (a_1^{u,d}, a_2^{u,d}, a_3^{u,d}, a_4^{u,d})$ are the projection coefficients found by matching to the large distance solutions. The matrices $M_{u,d}$ are defined by the asymptotic Z-string continuum solutions,

$$M_{u,d} = \begin{pmatrix} J_{|\nu|}(kR_o) & 0 & N_{|\nu|}(kR_o) & 0 \\ \mp \frac{E}{k} J_{|\nu|\pm 1}(kR_o) & \mp \frac{g}{k} J_{|\nu|\pm 1}(kR_o) & \mp \frac{E}{k} N_{|\nu|\pm 1}(kR_o) & \mp \frac{g}{k} N_{|\nu|\pm 1}(kR_o) \\ 0 & J_{|\nu|}(kR_o) & 0 & N_{|\nu|}(kR_o) \\ \pm \frac{g}{k} J_{|\nu|\pm 1}(kR_o) & \pm \frac{E}{k} J_{|\nu|\pm 1}(kR_o) & \pm \frac{g}{k} N_{|\nu|\pm 1}(kR_o) & \pm \frac{E}{k} N_{|\nu|\pm 1}(kR_o) \end{pmatrix}, \quad (98)$$

where the appropriate subscript must be placed on both ν and k ,

$$\nu_u = n + \alpha_L^u, \quad \nu_d = n + 1 + \alpha_L^d, \quad E^2 = k_{u,d}^2 + g_{u,d}^2.$$

By numerically solving the profile equations (89) to (96), each of the regular short distance spinors, \vec{S}_i , can evolved out to some sufficiently large distance, R , and matched to the asymptotic solutions. If we collect the up and down quark components into individual 4 component spinors, $\vec{V}_u(R)$ and $\vec{V}_d(R)$ respectively, we have,

$$\vec{V}_u = S_u \vec{\alpha}, \quad \vec{V}_d = S_d \vec{\alpha}, \quad (99)$$

where $\alpha^T = (\alpha_1, \alpha_2, \alpha_3, \alpha_4)$ and the scattering data is encoded in the matrices, $S_{u,d}$,

$$S_{u,d} = \begin{pmatrix} \psi_{1,1}^{u,d} & \psi_{1,2}^{u,d} & \psi_{1,3}^{u,d} & \psi_{1,4}^{u,d} \\ \psi_{2,1}^{u,d} & \psi_{2,2}^{u,d} & \psi_{2,3}^{u,d} & \psi_{2,4}^{u,d} \\ \psi_{3,1}^{u,d} & \psi_{3,2}^{u,d} & \psi_{3,3}^{u,d} & \psi_{3,4}^{u,d} \\ \psi_{4,1}^{u,d} & \psi_{4,2}^{u,d} & \psi_{4,3}^{u,d} & \psi_{4,4}^{u,d} \end{pmatrix}.$$

Here $\psi_{i,j}^{u,d}$ is the value of the i -th component of the up/down quark spinor at $r = R$ found by evolving the j -th regular short distance solution. From (97) the 4 component spinors \vec{V}_u and \vec{V}_d can be written as,

$$\begin{pmatrix} \vec{V}_u \\ \vec{V}_d \end{pmatrix} = \begin{pmatrix} M_u & 0 \\ 0 & M_d \end{pmatrix} \begin{pmatrix} \vec{a}_u \\ \vec{a}_d \end{pmatrix}. \quad (100)$$

By eliminating $\vec{\alpha}$ using (99), we can express \vec{a}_u or \vec{a}_d in terms of the other,

$$\vec{a}_d = M\vec{a}_u, \quad (101)$$

where,

$$M = M_d^{-1}S_dS_u^{-1}M_u. \quad (102)$$

Thus only 4 out of the 8 asymptotic projection coefficients are linearly independent. We arbitrarily treat the components of \vec{a}_u as our arbitrary coefficients. These degrees of freedom are of course related to the components of $\vec{\alpha}$. In fact, there are only 3 degrees of freedom because the spinor is only defined up to an overall normalisation constant.

As with the pure Z-string, the next step is to discretise the continuum by imposing boundary conditions on the spinor profiles at $r = R_o$. We *double up* the conditions used for the pure Z-string, this allows much of the technology developed in section 6 to be applied to the perturbed string. Specifically we set the first, third, fifth and seventh components of the 8 component spinor to zero at $r = R_o$. Clearly as the perturbation is switched off these conditions become identical to those used in the case of the unperturbed string.

Applying the boundary conditions at R_0 we find,

$$\frac{J_{|\nu_u|}(k_u R_o)}{N_{|\nu_u|}(k_u R_o)} = -\frac{a_3^u}{a_1^u} = -\frac{a_4^u}{a_2^u}, \quad (103)$$

and,

$$\frac{J_{|\nu_d|}(k_d R_o)}{N_{|\nu_d|}(k_d R_o)} = -\frac{a_3^d}{a_1^d} = -\frac{a_4^d}{a_2^d}. \quad (104)$$

Individually (103) and (104) are identical in nature to the discretisation conditions which arose in the case of the pure Z-string. However (103) and (104) must be solved simultaneously due to the non-trivial coupling between the up and down quarks induced by the upper component of the Higgs field.

We seek a discretisation condition of the form,

$$\frac{J_{|\nu|}(k_u R_o)}{N_{|\nu|}(k_u R_o)} = -X(k),$$

in order to employ the methodology developed in section 6. From (101) we have,

$$\frac{a_3^d}{a_1^d} = \frac{M_{3,1}\frac{a_1^u}{a_2^u} + M_{3,2} + M_{3,3}\frac{a_1^u}{a_2^u}\frac{a_4^u}{a_2^u} + M_{3,4}\frac{a_4^u}{a_2^u}}{M_{1,1}\frac{a_1^u}{a_2^u} + M_{1,2} + M_{1,3}\frac{a_1^u}{a_2^u}\frac{a_4^u}{a_2^u} + M_{1,4}\frac{a_4^u}{a_2^u}}, \quad (105)$$

and

$$\frac{a_4^d}{a_2^d} = \frac{M_{4,1}\frac{a_1^u}{a_2^u} + M_{4,2} + M_{4,3}\frac{a_1^u}{a_2^u}\frac{a_4^u}{a_2^u} + M_{4,4}\frac{a_4^u}{a_2^u}}{M_{2,1}\frac{a_1^u}{a_2^u} + M_{2,2} + M_{2,3}\frac{a_1^u}{a_2^u}\frac{a_4^u}{a_2^u} + M_{2,4}\frac{a_4^u}{a_2^u}}, \quad (106)$$

where a_3^u has also been eliminated using (103).

Implementing part of (104) by equating (105) with (106), we find a quadratic equation for $\frac{a_4^u}{a_2^u}$, thus we can consider $\frac{a_4^u}{a_2^u}$ to be a function of $\frac{a_4^u}{a_2^u}$. Substituting the solutions of this quadratic into (105) and (106), the energy of the continuum states and the ratio $\frac{a_4^u}{a_2^u}$ are the only remaining independent degrees of freedom. We must now impose the 2 remaining constraints,

$$\frac{J_{|\nu_u|}(k_u R_o)}{N_{|\nu_u|}(k_u R_o)} = -\frac{a_4^u}{a_2^u} \quad \text{and} \quad \frac{J_{|\nu_d|}(k_d R_o)}{N_{|\nu_d|}(k_d R_o)} = -\frac{a_3^d}{a_1^d}, \quad (107)$$

to determine the allowed energy E and the ratio $\frac{a_4^u}{a_2^u}$.

A solution to this system has only been found for degenerate masses, $g_u = g_d$ and hence $k_u = k_d$. For degenerate masses and $kR_o \gg 1$, using the standard large distance expansions of the Bessel functions, we have,

$$\cot(kR_o - \theta_u) = -\frac{a_4^u}{a_2^u}, \quad \cot(kR_o - \theta_d) = -\frac{a_3^d}{a_1^d},$$

where,

$$\theta_{u,d} = \frac{\pi}{2} \left(|\nu_{u,d}| + \frac{1}{2} \right). \quad (108)$$

Using standard trigonometric identities to eliminate kR_o gives,

$$\frac{\frac{a_4^u}{a_2^u} + \tan \theta_u}{\frac{a_4^u}{a_2^u} \tan \theta_u - 1} - \frac{\frac{a_3^d}{a_1^d} + \tan \theta_d}{\frac{a_3^d}{a_1^d} \tan \theta_d - 1} = 0. \quad (109)$$

The only independent variable in (109) is the ratio $\frac{a_4^u}{a_2^u}$ and we have a one dimensional root finding problem. This process, although conceptually straightforward, requires a significant amount of computational effort due to the singularities found in (109). Numerically solving (109) for a range of continuum energy values produces functions $\frac{a_4^u}{a_2^u}(E)$ which can then be used in (103) to provide a discretisation condition of a similar nature to that of the pure Z-string.

For a given value of the energy, 4 solutions of (109) are expected. Denoting these solutions by $X^\alpha(k)$ where $\alpha = 1, 2, 3, 4$, for $kR_o \gg 1$ the discretisation condition reads,

$$\cot(kR_o - \theta_u) = -X^\alpha(k), \quad (110)$$

which can be inverted using (52) to give,

$$k_i R_o = i\pi + \beta_\infty^\alpha \pi + \theta_u + \cot^{-1}(-X^\alpha(k)) \Big|_P^{cont}, \quad (111)$$

with the value of β_∞^α given by (156).

Using the analysis of section 6, the continuum contribution to the fermionic energy of the perturbed string made by a given angular momentum mode is,

$$\begin{aligned}
E_{cont}^n(\tau) &= \frac{R_o}{\pi^2} \int_{\tau}^{\infty} \frac{dt}{t^2} e^{-tg^2} \int_o^{\infty} dk e^{-tk^2} - \frac{1}{2\pi} \int_{\tau}^{\infty} \frac{dt}{t^2} e^{-tg^2} \\
&- \frac{1}{4\pi} \sum_{\alpha=1}^4 \beta_{\infty}^{n,\alpha} \int_{\tau}^{\infty} \frac{dt}{t^2} e^{-tg^2} - \frac{\theta_u}{\pi^2} \int_{\tau}^{\infty} \frac{dt}{t^2} e^{-tg^2} \\
&- \frac{1}{2\pi^2} \int_{\tau}^{\infty} \frac{dt}{t} e^{-tg^2} \int_0^{\infty} dk k e^{-tk^2} \sum_{\alpha=1}^4 \cot^{-1}(-X^{n,\alpha}(k)) \Big|_p^{cont}. \quad (112)
\end{aligned}$$

As in the case of the unperturbed string, the first two terms cancel when two systems are compared.

We must also consider the bound states of the perturbed string by looking for suitable linear combinations of the regular short distance spinors that match, at large radial distances, to spinor profiles that decay exponentially. In the perturbed string there are 4 regular short distance spinors in each mode, we denote these by \vec{S}_i . The perturbations we are considering are localised to the string core so, just as in the case of the continuum, the 8 linearly independent large distance solutions are the same as those which arose in the case of the unperturbed string (41).

As in the continuum, we have a doubling up of states and matching conditions. The existence of a massive bound state solution requires that the coefficients of the exponentially divergent solutions vanish when a suitable short distance spinor is evolved to large distance. Taking a general linear combination of the 4 regular short distance spinors gives the bound state condition,

$$\alpha_i a_{i,1}^u = \alpha_i a_{i,2}^u = \alpha_i a_{i,1}^d = \alpha_i a_{i,2}^d = 0, \quad (113)$$

where the summation convention is used and the asymptotic states are defined in (41). These conditions lead to the determinant equation,

$$\begin{vmatrix}
a_{1,1}^u & a_{2,1}^u & a_{3,1}^u & a_{4,1}^u \\
a_{1,2}^u & a_{2,2}^u & a_{3,2}^u & a_{4,2}^u \\
a_{1,1}^d & a_{2,1}^d & a_{3,1}^d & a_{4,1}^d \\
a_{1,2}^d & a_{2,d}^d & a_{3,2}^d & a_{4,2}^d
\end{vmatrix} = 0. \quad (114)$$

We find two bound states in the perturbed string background,

$$E^{n=-1} = 0.0505, \quad E^{n=0} = 0.9992. \quad (115)$$

$n = -1$ corresponds to the mode in which the up and down quark zero modes reside if the perturbation is switched off, thus, as first shown in [12], the perturbation lifts the energy of the zero modes to form a low energy bound state. The index theorem [20] which ensures that there are zero mode solutions in the

background of the pure Z-string no longer applies because the perturbation in the upper component of the Higgs field is exactly one of the fields which makes the electroweak string non-topological. In terms of the spectral flow of fermion energy levels, as the perturbation in the upper component of the Higgs field is turned on, the up and down quark zero modes, which are restricted to move in opposite directions along the length of the string, are combined to form a low energy massive bound state. The number of fermionic degrees of freedom associated with the zero modes is therefore unchanged. Similar behaviour has been observed in the context of GUT string zero modes mixing with massless modes [30].

Denoting the set of massive bound state solutions in a given mode by $\{E_{n,i}\}$, the total contribution made by the mode to the fermionic energy becomes,

$$\begin{aligned}
E_{fermion}^n(\tau) &= \frac{R_o}{\pi^2} \int_{\tau}^{\infty} \frac{dt}{t} e^{-tg^2} \int_0^{\infty} dk e^{-tk^2} - \frac{1}{2\pi} \int_{\tau}^{\infty} \frac{dt}{t^2} e^{-tg^2} \\
&+ \frac{1}{4\pi} \int_{\tau}^{\infty} \frac{dt}{t^2} \sum_i e^{-tE_{n,i}^2} - \frac{1}{4\pi} \sum_{\alpha=1}^4 \beta_{\infty}^{n,\alpha} \int_{\tau}^{\infty} \frac{dt}{t^2} e^{-tg^2} - \frac{\theta_u}{\pi^2} \int_{\tau}^{\infty} \frac{dt}{t^2} e^{-tg^2} \\
&- \frac{1}{2\pi^2} \int_{\tau}^{\infty} \frac{dt}{t} e^{-tg^2} \int_0^{\infty} dk k e^{-tk^2} \sum_{\alpha=1}^4 \cot^{-1}(-X^{n,\alpha}(k)) \Big|_p^{cont}. \quad (116)
\end{aligned}$$

9.3 The Perturbed String Counter Term

The calculation of the counter term for the perturbed string proceeds along the same lines as the corresponding calculation for the pure Z-string. The 4 component Z-string Dirac Hamiltonian is replaced by the 8 component Dirac Hamiltonian defined in (87). The counter term is the sum of the individual up and down quark counter terms in the background of the pure Z-string (as defined by (64), (65) and (63)) together with some modification arising from the perturbation.

By squaring the Hamiltonian in (87) and writing it in the form,

$$\hat{H}^2 = -(\partial_i + \Gamma_i)(\partial_i + \Gamma_i) + a(x), \quad (117)$$

we can apply the formalism for the heat kernel expansion developed in section 7. Explicitly we have,

$$\Gamma_i = iqZ_i \text{diag} \left(\alpha_R^u I_{2 \times 2}, -\alpha_L^u I_{2 \times 2}, \alpha_R^d I_{2 \times 2}, -\alpha_L^d I_{2 \times 2} \right), \quad (118)$$

and,

$$a(x) = \begin{pmatrix} a_u(x) & a_I(x) \\ a_I^\dagger(x) & a_d(x) \end{pmatrix}, \quad (119)$$

where,

$$a_u(x) = \begin{pmatrix} -iq\alpha_R^u(\partial_i Z_i - \sigma^j \sigma^i \partial_i Z_j) & ig_u \sigma^i \partial_i (f(r) e^{i\theta}) \\ +g_u^2 f(r)^2 + g_u^2 g(r)^2 & -g_u q \sigma^i Z_i f(r) e^{i\theta} \\ -ig_u \sigma^i \partial_i (f(r) e^{-i\theta}) & iq\alpha_L^u(\partial_i Z_i - \sigma^j \sigma^i \partial_i Z_j) \\ -g_u q \sigma^i Z_i f(r) e^{-i\theta} & +g_u^2 f(r)^2 + g_u^2 g(r)^2 \end{pmatrix}, \quad (120)$$

$$a_d(x) = \begin{pmatrix} -iq\alpha_R^d(\partial_i Z_i - \sigma^j \sigma^i \partial_i Z_j) & ig_d \sigma^i \partial_i (f(r) e^{-i\theta}) \\ +g_d^2 f(r)^2 + g_d^2 g(r)^2 & +g_d q \sigma^i Z_i f(r) e^{-i\theta} \\ -ig_d \sigma^i \partial_i (f(r) e^{i\theta}) & iq\alpha_L^d(\partial_i Z_i - \sigma^j \sigma^i \partial_i Z_j) \\ +g_d q \sigma^i Z_i f(r) e^{i\theta} & +g_d^2 f(r)^2 + g_d^2 g(r)^2 \end{pmatrix}, \quad (121)$$

and,

$$a_I(x) = \begin{pmatrix} 0 & g_u q g(r) \sigma^i Z_i (\alpha_R^u + \alpha_L^d) \\ & -ig_u \sigma^i \partial_i g(r) \\ -ig_d g(r) \sigma^i \partial_i g(r) & \\ -q g_d g(r) \sigma^i Z_i (\alpha_R^d + \alpha_L^u) & (g_d^2 - g_u^2) g(r) f(r) e^{-i\theta} \end{pmatrix}. \quad (122)$$

After a similar, but more lengthy, calculation to that presented in appendix B, we find the heat kernel coefficients in the perturbed string background are,

$$\text{Tr}[a_1] = -4(g_u^2 + g_d^2)(f(r)^2 + g(r)^2), \quad (123)$$

and,

$$\begin{aligned} \text{Tr}[a_2] = & \frac{2}{3}(\alpha_R^u + \alpha_L^u + \alpha_R^d + \alpha_L^d) \left(\frac{\nu(r)'}{r} \right)^2 \\ & + (g_u^2 f(r)^2 + g_d^2 g(r)^2)^2 + (g_u^2 f(r)^2 + g_u^2 g(r)^2)^2 \\ & + (g_d^2 f(r)^2 + g_u^2 g(r)^2)^2 + (g_d^2 f(r)^2 + g_d^2 g(r)^2)^2 \\ & + 2(g_u^2 + g_d^2) \left((f(r)')^2 + \left(\frac{f(r)[\nu(r) + 1]}{r} \right)^2 \right) + 2(g_d^2 - g_u^2)^2 g(r)^2 f(r)^2 \\ & + 2g_u^2 \left((g(r)')^2 + (\alpha_R^u + \alpha_L^d)^2 \left(\frac{\nu(r)g(r)}{r} \right)^2 \right) \\ & + 2g_d^2 \left((g(r)')^2 + (\alpha_R^d + \alpha_L^u)^2 \left(\frac{\nu(r)g(r)}{r} \right)^2 \right). \end{aligned} \quad (124)$$

We see that (123) and (124) reduce to the sum of the individual contributions made by the up and down quark in the background of the unperturbed string when the perturbation is set to zero.

Having found expressions for both the fermionic energy of the perturbed string and the corresponding counter term, these results can be combined with the corresponding calculations for the unperturbed string to compare the fermionic energy of a perturbed string to that of an unperturbed string.

9.4 The Change in the Ground State Energy

In order to obtain a well behaved mode decomposition of the energy difference, we must examine the angular dependence of the spinors. The space spanned by the n th modes of the perturbed string energy eigenstates (88) is also spanned by the set formed by the union of the $(n + 1)$ th up quark modes and the n th down quark modes in the background of the unperturbed string, as defined by (29). Physically this means that the spectral flow caused by the perturbation only mixes the $(n + 1)$ th up quark mode and the n th down quark mode. Thus the energy difference is found by subtracting the sum of the contributions made by the $(n + 1)$ th up quark mode and the n th down quark mode in the background of the unperturbed string from the contribution made by the n th perturbed string mode. Matching modes in this manner ensures that the fermionic states of the two systems can be put into a 1 : 1 correspondence.

This coupling of modes is consistent with the mixing of the up quark zero mode ($n = -1$) and the down quark zero mode ($n = 0$).

Given this coupling of the modes, it is convenient to make the following mapping on the unperturbed up quark mode number which was used in section 4,

$$n_u \Rightarrow n - 1.$$

Again we split the energy difference into a bound state contribution and a continuum contribution. For the bound states we have,

$$\begin{aligned} \delta E_{bound}^n(\tau) = & -\frac{(\alpha_{ZM,d}^n + \alpha_{ZM,u}^n)}{8\pi\tau} + \frac{1}{4\pi} \sum_i \left((E_{n,i}^P)^2 \Gamma(-1, \tau(E_{n,i}^P)^2) \right. \\ & \left. - (E_{n,i}^d)^2 \Gamma(-1, \tau(E_{n,i}^d)^2) - (E_{n,i}^u)^2 \Gamma(-1, \tau(E_{n,i}^u)^2) \right) \\ & - \frac{1}{4\pi} \left(\sum_{\alpha=1}^4 \beta_{\infty,P}^{n,\alpha} - \sum_{\pm} \beta_{\infty,d}^{n,\pm} - \sum_{\pm} \beta_{\infty,u}^{n,\pm} \right) g^2 \Gamma(-1, g^2\tau), \quad (125) \end{aligned}$$

where $\{E_{n,i}^P\}$, $\{E_{n,i}^d\}$ and $\{E_{n,i}^u\}$ are the set of positive energy massive bound state solutions for the perturbed string, down quark and up quark respectively with mode number n . $\alpha_{ZM,u}^n$ and $\alpha_{ZM,d}^n$ denote the number of up and down quark zero mode solutions respectively in the unperturbed background with mode number n . The values of the integers β_{∞} required to fix the discretisation condition uniquely at large momentum, are determined by counting the singularities in the functions $X(k)$ and using (156).

The continuum contribution to the energy difference is given by,

$$\begin{aligned} \delta E_{cont}^n(\tau) &= -\frac{1}{2\pi^2}(\theta_{\nu_u} - \theta_{\nu_d}) \int_{\tau}^{\infty} \frac{dt}{t^2} e^{-tg^2} \\ &\quad -\frac{1}{2\pi^2} \int_{\tau}^{\infty} \frac{dt}{t} e^{-tg^2} \int_0^{\infty} dk k e^{-tk^2} \left(\sum_{\alpha=1}^4 \cot^{-1}(-X^{n,\alpha}(k)) \Big|_p^{cont} \right. \\ &\quad \left. - \sum_{\pm} \cot^{-1}(-X^{n,d}(k)) \Big|_p^{cont} - \sum_{\pm} \cot^{-1}(-X^{n,u}(k)) \Big|_p^{cont} \right). \end{aligned} \quad (126)$$

The second term in (126) is of a familiar form, while the first is a new feature of the perturbed string. Treating $\frac{a_4^u}{a_2^u}$ as the independent variable gives a discretisation condition of the form in (111). This has the same form as the discretisation condition for the up quark in the unperturbed string background. Had we used $\frac{a_3^d}{a_1^d}$ as the independent variable instead, the discretisation condition would have taken the form,

$$k_i R_o = i\pi + \beta_{\infty}\pi + \theta_{\nu_d} + \cot^{-1}(-X(k)) \Big|_p^{cont},$$

which is of the same form as the discretisation condition of the down quark in the unperturbed string background. Thus, by working with $\frac{a_4^u}{a_2^u}$, we are taking the up quark states of the unperturbed string as our reference points in both sectors. The first term in (126) represents the shifts of the down quark states of the unperturbed string relative to these up quark reference points. There are of course corresponding factors within the perturbed string phase shifts, so that overall the energy difference is independent of the reference points used. It is most natural to absorb this term into the integral over the continuum momentum. Using (108) it is easily seen that,

$$\theta_{\nu_u} - \theta_{\nu_d} = \frac{\pi}{2}(|\nu_u| - |\nu_d|), \quad (127)$$

and so,

$$\delta E_{cont}^n = -\frac{1}{2\pi^2} \int_0^{\infty} dk k \Gamma(0, \tau(k^2 + g^2)) F^n(k), \quad (128)$$

where,

$$\begin{aligned} F^n(k) &= \sum_{\alpha=1}^2 \cot^{-1}(-X_{p,n}^{\alpha}(k)) \Big|_p^{cont} - \sum_{\pm} \cot^{-1}(-X_{d,n}^{\pm}(k)) \Big|_p^{cont} \\ &\quad - \sum_{\pm} \cot^{-1}(-X_{u,n}^{\pm}(k)) \Big|_p^{cont} - \pi(|\nu_d| - |\nu_u|). \end{aligned} \quad (129)$$

After some simplification, the counter term for the energy difference is given by,

$$E_{CT}(\tau, \mu) = \frac{1}{16\pi} \int_0^{\infty} dr r \left(\left(\frac{1}{\tau} - \frac{1}{\mu} \right) \Delta[a_1] + \log\left(\frac{\mu}{\tau}\right) \Delta[a_2] \right), \quad (130)$$

where,

$$\Delta[a_1] = -4(g_u^2 + g_d^2)g(r)^2, \quad (131)$$

and,

$$\begin{aligned} \Delta[a_2] = & 2(g_u^4 + d_d^4)(g(r)^4 + 2f(r)^2g(r)^2) + 2(g_u^2 + g_d^2)(g'(r))^2 \\ & + 2\left(g_u^2(\alpha_R^u + \alpha_L^d)^2 + g_d^2(\alpha_R^d + \alpha_L^u)^2\right) \left(\frac{\nu(r)g(r)}{r}\right)^2. \end{aligned} \quad (132)$$

The degenerate mass case under consideration is obtained by simply putting $g_u = g_d = g$ in (131) and (132).

The counter term in (130) still contains the arbitrary scale μ . As discussed in section 7, the total energy is independent of the particular value of μ because the parameters in the theory also depend upon μ in exactly the manner to ensure that physical quantities are independent of μ . The value of μ is set by the typical energy scale in the problem, which we take to be the mass of the Z boson. By fixing the vacuum expectation value of the Higgs field to be $\nu = 247$ GeV, we have,

$$M_z = \frac{76.9 \text{ GeV}}{|\sin 2\theta_w|}. \quad (133)$$

Taking $\theta_w = 0.5$, we have $M_z \approx 0.311$ in units of the vacuum expectation value, giving,

$$\mu = \frac{1}{M_z^2} \approx 10.32. \quad (134)$$

Finally, performing the integral in (130) for the profile functions shown in figure 6, we find that the counter term is given by,

$$E_{CT}(\tau) = a_1 \left(\frac{1}{\tau} - 10.34\right) + a_2 \log\left(\frac{10.34}{\tau}\right), \quad (135)$$

where,

$$a_1 = -3.97886 \times 10^{-4}, \quad a_2 = 5.76546 \times 10^{-4}. \quad (136)$$

The specific parameter values used in the calculation were,

$$\theta_w = 0.5, \quad g_u = g_d = 1.0, \quad \beta = \frac{M_H}{M_Z} = 0.943. \quad (137)$$

The actual background profile are shown in figure 6. The Higgs and gauge field profile equations $f(r)$ and $\nu(r)$ were found by solving the Nielsen Olesen equation (10), (11) for the parameters given above using numerical relaxation [31]. The perturbation in the upper component of the Higgs field was taken to be a standard gaussian function, so that it is non-zero inside the core of the string but decays rapidly outside the core;

$$g(r) = 0.1e^{-r^2}. \quad (138)$$

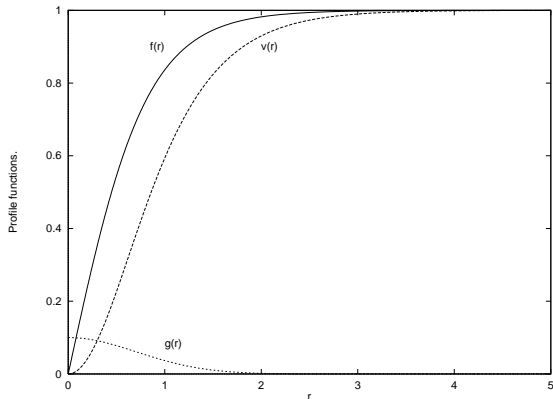


Figure 6: The background profile functions used.

As discussed above, we find two massive bound state solutions in the background on the perturbed string. The energies of these bound states are found to be,

$$E_{n=0}^P = 0.99918, \quad E_{n=-1}^P = 0.0505. \quad (139)$$

In the background of the unperturbed string the only massive bound state is a down quark bound state with $n = 0$ and energy,

$$E_{n=0}^d = 0.99918. \quad (140)$$

This energy is, to this accuracy, identical to that of the massive bound state in the $n = 0$ mode in the perturbed string background. Hence these two state are naturally paired in the bound state energy contribution.

The zero modes that appear in the pure Z-string background naturally pair up with the low energy, $n = -1$, massive bound state in the perturbed string background.

Given this natural pairing of the bound states, all the other contributions in (125) should vanish for each n . That is,

$$\sum_{\alpha=1}^4 \beta_{\infty,P}^{n,\alpha} - \sum_{\pm} \beta_{\infty,d}^{n,\pm} - \sum_{\pm} \beta_{\infty,u}^{n,\pm} = 0, \quad (141)$$

where the values of the integers β are determined by the singularities of the functions $X^n(k)$ through (156). This is indeed found to be the case. Physically this means that in the spectral flow between the unperturbed string and the perturbed string, no continuum states drop below threshold energy to become massive bound states. In accordance with Levinson's theorem, $F^n(k=0) = 0$ for

all values of n , as there is no difference in the number of bound states between the two systems.

The functions $F^n(k)$ that define the shift in the energy of the continuum states are defined by (129). They have been found numerically using the formalism developed in sections 3-6. Figure 7 shows plots of the functions $F^n(k)$ for $n = 0, 1, 2, 3, 4, 5$, similar behaviour is found for negative n .

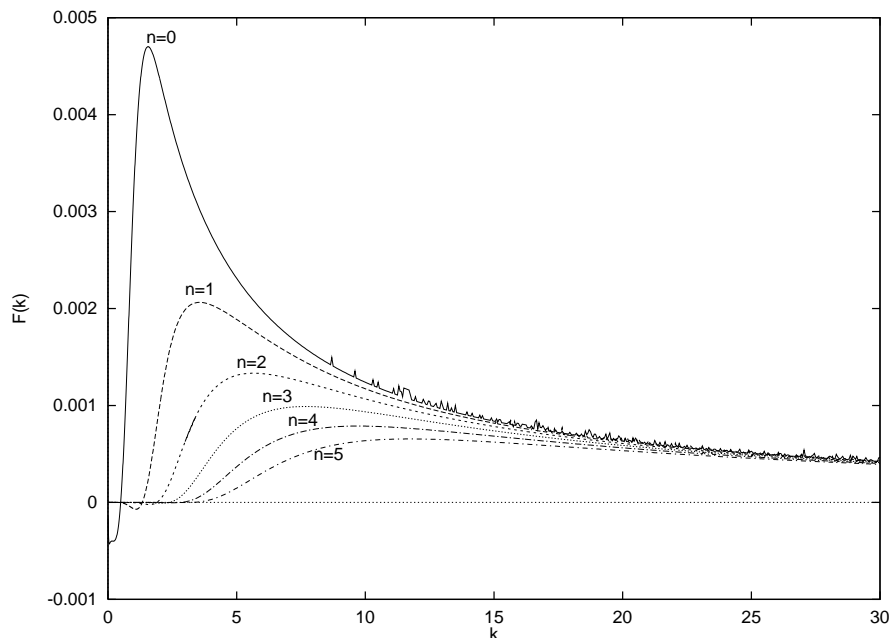


Figure 7: The functions $F^n(k)$ for $n = 0, 1, 2, 3, 4, 5$.

There are a number of features of the functions $F^n(k)$ worth noting: Except for a small range around zero momentum, the functions $F^n(k)$ are positive for all values of n . All other factors comprising the integrand for the continuum contribution for each mode are positive definite. However there is an overall minus sign, so each mode contributes a negative definite amount to the regularised fermionic energy.

The values of $F^n(k = 0)$ are indeed zero for all n (closer inspection of the behaviour of $F^0(k)$ for small k reveals the function does indeed vanish).

The functions $F^n(k)$ are *enveloped* by the functions with smaller absolute mode number. As all the other factors in the integrand for the energy contribution are independent of n , this implies that as the absolute value of the mode number increases the contribution made by the modes to the regularised continuum energy decrease.

In units of the Higgs VEV, $F^n(k) \sim 0$ for k less than about the absolute value of n . This behaviour was noted in the case of the core model and is the key to

the convergence with n . Physically, as the spinors with high angular momentum are small within the core of the string for this range of momenta, they do not couple strongly to the perturbation.

The functions $F^n(k)$ die away as k becomes large. Numerical fitting to a function of the form $\frac{a_1}{k} + \frac{a_2}{k^2} + \dots$ suggests a $\frac{1}{k}$ fall off.

We can now perform the integrals in (128) for specific values of the cut-off τ and obtain the regularised fermionic energy. Numerically, the most intensive part of the calculation is the production of the functions $F^n(k)$. These functions were tabulated for n between -20 and 20 .

Figure 8 shows the continuum contribution to the fermionic energy made by each angular mode for n between -10 and 10 and for three values of the regulator τ . We see that the contribution made by each mode rapidly decreases as the absolute value of the mode number increases, this implies rapid convergence of the the sum over n . However, as $\tau \rightarrow 0$, the contributions from the low n modes can be seen to get larger, the fall off as $|n|$ gets larger is slower, and more terms must be included in the sum over n , as discussed in section 8.4.

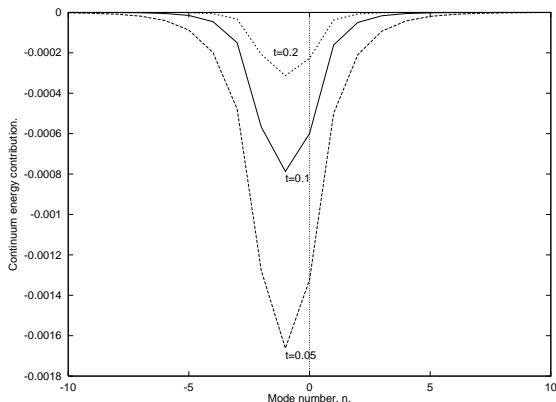


Figure 8: A plot of $\delta E_{cont}^n(\tau)$ as a function of n for $\tau = 0.2, 0.1, 0.05$.

We find the regularised fermionic energy for a given value of τ by adding together the contributions made by the bound states and the continuum in each mode and then summing over a sufficient number of mode to ensure convergence. The renormalised fermionic energy is then obtained by subtracting the counter term.

There are several sources of numerical error in this calculation. These arise due to truncation of the sum over angular modes, truncation of the momentum integral, finite tabulation density of the functions $F^n(k)$ and numerical errors in the values of these functions.

The first two errors limit how small the cut off τ can be taken. Figure 9 shows the regularised continuum energy scaled by the cut off as a function of the cut

off for three different values of the maximum absolute value of the mode number taken in the sum. As the number of modes included in the sum decreases, the continuum contribution to the regularised fermionic energy becomes less negative. As the contribution made by each mode to the regularised energy is negative definite, the truncation in the sum over n induces a systematic error in the total regularised fermionic energy. As the number of modes included increases, τ can be reduced further before significant errors arise.

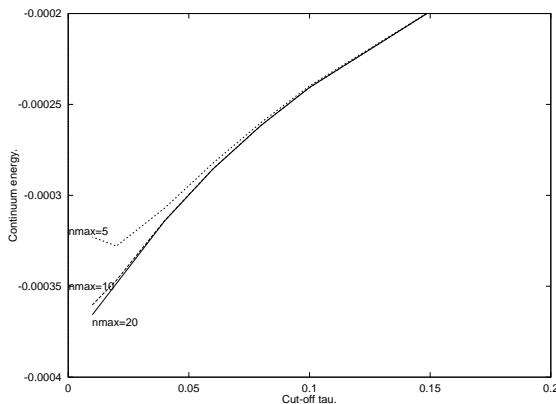


Figure 9: Plots of $\tau\delta E_{cont}(\tau)$ as a function of τ for different truncations in the sum over the mode number n .

As discussed in section 8.4, the combination of the regulating factor, e^{-tk^2} , and the fact that the functions $F^n(k)$ are small for $k < n$, leads to an exponential suppression of the contribution from high angular modes by a factor of the form, $e^{-\tau n^2}$. For a maximum mode number of 20 and a suppression factor of order tol , the smallest value of τ which can be used with confidence is given by,

$$\tau \approx \frac{\log(tol)}{-400}. \quad (142)$$

To quantify the errors arising from the integral over the momentum we varied the interpolation procedure and the tabulation density. Second and third order polynomials were used to interpolate between the tabulated points and a second order polynomial fit was made to only half the data points. The error was then estimated from the maximum absolute difference between these three methods. Again the error increases as the cut-off is taken away.

The tabulation density used, the truncation $k_{max} = 50$ and the truncation $n_{max} = 20$ all lead to errors of order 10^{-6} at $\tau \approx 0.04$. For smaller τ values the errors grow rapidly.

Using a quadratic fit to the nodes with $\tau \geq 0.04$ and extrapolating to $\tau = 0$, we find,

$$\delta E_{fermion} = -0.0033 \pm 0.00002, \quad (143)$$

where the error has been estimated by fitting to fewer nodes.

We have an explicit calculation of the difference between the fermionic ground state energies of the perturbed string and the unperturbed string. This energy difference is negative, as conjectured by Naculich [12]. The filled Dirac sea further destabilises the string with respect to a perturbation of this type.

9.5 Scaling With Perturbation Size

Repeating this calculation for a perturbation that is five times larger than the previous one, we find the same number of bound states and that the functions $F^n(k)$ have the same characteristic features but larger typical values. The typical increase in these values is of the same order as the increase in the perturbation squared (i.e. ~ 25).

Figure 10 shows a plot of the renormalised energy at a function of the cut-off. The extrapolation to obtain the value of the fermionic energy was again carried using a quadratic fit. The renormalised fermionic energy is found to be,

$$\delta E_{fermion} = -0.0667 \pm 0.0002. \quad (144)$$

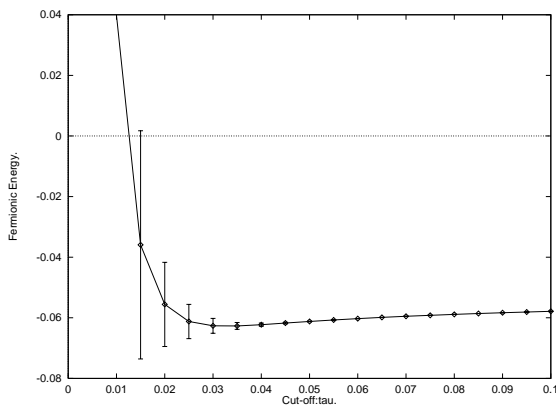


Figure 10: A plot of the renormalised fermionic energy $\delta E_{ren}(\tau)$ for the larger perturbation.

Again the fermionic energy can be seen to be negative and hence does not stabilize the Z-string.

Comparing the magnitudes of the two fermionic energy shifts, we see that the effect has increased by roughly the same order as the increase in the perturbation squared (i.e. ~ 25). This is consistent with the suggestions of Naculich [12].

We have calculated the renormalised fermionic energy difference between the perturbed and pure Z-string. In both cases the fermionic energy is found to be negative and hence has a destabilizing effect on the string. Our values appear to scale roughly with the square of the magnitude of the perturbation.

9.6 Populating Positive Energy States

Having calculated the energy shift of the fermionic vacuum, we can now consider the effects of populating positive energy bound states. The inclusion of positive energy bound states is fairly straightforward, the positive energy states are filled up to some given value of the momentum along the length of the string, \tilde{k} . As the perturbation increases, the energy of these states tends to increase and the extra contribution to the fermionic energy shift will be positive. At some value of \tilde{k} the contributions from the fermionic ground state and the populated positive energy bound states cancel. In this situation the fermionic energy has a neutral effect on the stability of the string. For higher values of \tilde{k} the overall energy shift is positive and the fermions enhance the stability of the string.

It was shown in section 3 that the fermionic contribution to the energy of a field configuration is given by,

$$\sum_r (-E_r + n_r E_r),$$

where the sum is over all the positive energy states and n_r is the occupation number of the positive energy states. If an adiabatic perturbation were turned on then the change in the fermionic energy is given by,

$$\delta E_{ferm} = \delta E_{sea} + \delta E_{pos},$$

where δE_{sea} is the sum of the shifts in the negative energy states computed above, and δE_{pos} is the shift in the energy of the occupied positive energy states. For an adiabatic change, the occupation numbers of the states remain constant and we have,

$$\delta E_{pos} = \sum_r n_r (E'_r - E_r),$$

where E'_r is the shifted value of E_r when the perturbation is switched on. In the spectral flow picture these state flow into one another.

In the case of the string the states of interest are the zero modes in the unperturbed string background and the low energy massive bound state which the up and down quark zero modes combine to become when the perturbation is turned on. These are the only states between which there is a significant energy shift.

We start in the pure Z-string background, with up quark zero mode states with momentum in the range $[0, \tilde{k}]$ filled, and down quark zero mode states with momentum in the range $[-\tilde{k}, 0]$ filled. In the perturbed string this gives low, positive energy bound states with an absolute momentum up to \tilde{k} filled. Figure 11 illustrates the population of positive states for the perturbed string (low energy massive bound state) and the unperturbed string (up and down quark zero modes) up to a value of $\tilde{k} = 2.5$. If the low energy bound state has mass δm , then

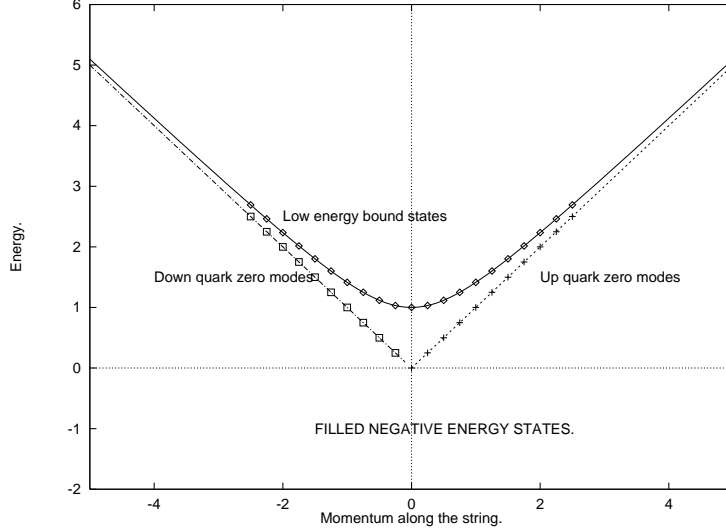


Figure 11: A typical scenario illustrating the population of positive energy states.

a state with momentum k_z along the string satisfies the mass-shell condition, $E^2 = k_z^2 + \delta m^2$. The zero modes move at the speed of light along the length of the string and therefore their energy, E , satisfies, $E = k_z$, as illustrated by the 45° zero mode lines in figure 11.

Discretising the momentum along the string as in section 5, we have,

$$\delta E_{pos} = \sum_{n=-n_{max}}^{n_{max}} \left[\sqrt{k_n^2 + \delta m^2} - |k_n| \right], \quad (145)$$

where, $k_n = \frac{2\pi n}{L}$, and L is the length of the cylindrical box we are considering. Taking L to infinity and defining the maximum momentum \tilde{k} by, $\tilde{k} = 2\pi n_{max}/L$, we obtain,

$$\begin{aligned} \delta E_{pos} &= \frac{1}{\pi} \int_0^{\tilde{k}} dk (\sqrt{k^2 + \delta m^2} - |k|) \\ &= \frac{\delta m^2}{2\pi} \left[\log\left(\frac{\tilde{k}}{\delta m} + \sqrt{1 + \frac{\tilde{k}^2}{\delta m^2}}\right) + \frac{\tilde{k}}{\delta m} \left(\sqrt{1 + \frac{\tilde{k}^2}{\delta m^2}} - \frac{\tilde{k}}{\delta m} \right) \right]. \end{aligned}$$

δE_{pos} is positive as expected, thus populated positive energy states help to stabilise the string.

There is also a shift in the energy of any massive bound states when the string is perturbed. The energy shift for these states is simply found by considering the (possibly fictitious) zero mode as a reference and taking the difference of calculated with the initial and final masses.

It may be possible to introduce a sufficient population of positive energy bound states and zero modes to stabilize the string against the negative curvature

induced by the Dirac sea and the bosonic instabilities. This question is considered in ref.[32].

10. Conclusions

We have systematically calculated the order \hbar fermionic energy shift when an electroweak string is perturbed. This calculation is the first to take into account the effects of the Dirac Sea. Our approach allows the infinite volume limit to be recovered analytically. We have developed a state counting procedure that correctly counts states flowing from the continuum to bound modes and allows the fermionic energy to be renormalised. The momentum shift functions we evaluate satisfy Levinson's theorem. Convergence of our numerical sums and the finiteness of the renormalised energy shifts have both been demonstrated.

The Dirac Sea energy shift when a pure Z-string is perturbed is found to be negative and scales roughly as the size of the perturbation squared. The Dirac Sea thus provides a term with negative curvature to the effective potential and has a destabilising effect on the string.

However, populated positive energy states have their energy increased by the perturbation and hence have a stabilising effect on the string. The total fermionic effect may vanish if there is a sufficient population of positive energy bound states on the string. A larger population of bound states leads to the fermions having a stabilising effect overall. This raises the fascinating possibility that electroweak strings may be stable if they carry a fermionic current.

Acknowledgements

The authors would like to thank G. Shore, S. Hands and N. Dorey for useful discussions. WBP would like to thank A.-C.Davis for useful discussions. MG would like to thank S.Naculich for useful discussions and acknowledge PPARC for a research studentship.

References

- [1] Y.Nambu, Nuc. Phys. B130 (1977) 505.
- [2] T.Vachaspati, Nuc. Phys. B397 (1993) 648.
- [3] M.Barriola, T.Vachaspati and M.Bucher, Phys. Rev. D50 (1994) 2819, N.F.Lepora and A.-C.Davis, Phys. Rev. D58 (1998) 125028.
- [4] T.W.B.Kibble, Phys. Rev. 155 (1967) 1554.
- [5] M.James, L.Perivoloropoulos and T.Vachaspati, Nuc. Phys. B395 (1993) 534.

- [6] M.Goodband and M.Hindmarsh, Phys. Lett. B363 (1995) 58.
- [7] T.Vachaspati and M.Barriola Phys. Rev. Lett. 69 (1992) 1867.
- [8] R.H.Brandenberger and A.-C.Davis, Phys. Lett. B308 (1993) 79.
- [9] M.A.Earnshaw and M.James Phys. Rev. D48 (1993) 5818
- [10] T.Vachaspati, and R.Watkins, Phys. Lett. B318 (1993) 318.
- [11] M.Nagasawa and R.Brandenberger, hep-ph/9904261.
- [12] S.Naculich, Phys. Rev. Lett. 75 (1995) 998; S.Kono, and S.Naculich, hep-ph/9507350.
- [13] L.Hong, and T.Vachaspati, Nuc. Phys. B470 (1996) 176.
- [14] H.B.Nielsen and P.Olesen, Nuc. Phys. B144, (1973) 376.
- [15] W.B.Perkins, Phys. Rev. D47 (1993) 5224.
- [16] A.Achucarro, G.Gregory, J.A.Harvey and K.Kuijken, Phys. Rev. Lett. 72 (1994) 3646.
- [17] M.Earnshaw, and W.B.Perkins, Phys. Lett. B328 (1994) 337.
- [18] Rajaraman, *Solitons and Instantons.*, North-Holland, 1982.
- [19] R.Jackiw and P.Rossi, Nuc. Phys. B190 (1981) 681.
- [20] E.J.Weinberg, E.J., Phys. Rev. D24 (1981) 2669.
- [21] I.S.Gradshiteyn and I.M.Ryzhik, *Table of integrals, series and products.*, Academic Press, 1963.
- [22] P.Ramond, *Field theory : A modern primer.*, Addison-Wesley Publishing Company, 1988.
- [23] S.A.Fulling, *Aspects of quantum field theory in curved space-time.* London Mathematical Society Student Texts, Cambridge University Press, 1985.
- [24] D.Diakonov et. al., Phys. Rev. D49 (1994) 6864.
- [25] A.C.Davis, A.P. Martin, and N.Ganoulis, Nuc. Phys. B419 (1994) 323.
- [26] M.Nagasawa, Astropart. Phys. 5 (1996) 231.
- [27] R.Jackiw, and C.Rebbi, Phys. Rev. D13 (1976) 3398.
- [28] A.J.Niemi and G.W.Semenoff, Phys. Rep. 3 (1986) 100.

- [29] N.Levinson, Kgl. Danske Videnskab, Mat.-fys. Medd. 25 (1949) 9; L.I.Schiff, *Quantum mechanics.*, McGraw-Hill, 1968; D.I.Diakonov, V.Y.Petrov and P.V.Pobylitsa, Nuc. Phys. B306 (1988) 809; N.Poliatzky, Phys. Rev. Lett. pg. 2507, Vol. 70, 1993.
- [30] S.C.Davis, A.-C.Davis and W.B.Perkins, Phys. Lett. B408 (1997) 81.
- [31] W.H.Press et. al., *Numerical Recipes in Fortran.*, Cambridge, 1992.
- [32] M.Groves and W.B.Perkins SWAT/228 *in preparation.*

Appendix A: Discretisation Of The Continuum

To carry out the sum over the continuum states we first impose conditions on the spinor profile functions on the surface of a cylinder of radius R_o centred on the core of the string. The conditions used select a discrete subset of the continuum states and we trace over this discrete set of states. The full continuum is recovered as $R_o \rightarrow \infty$. This can be done analytically, so that the actual trace over the continuum can then be done in the physical, infinite volume limit. The use of the discretisation condition is merely an intermediate step in setting up the sum over the continuum states, it is critical as it ensures that the correct density of states is used.

To discretise the continuum we demand that the 1st and 3rd components of the spinors vanish at some large radial distance $r = R_o$. The physical answer clearly should not depend in anyway upon the discretisation condition used and alternatives could have been used. The critical point is that as R_o is taken to infinity, the full continuum should be recovered, so all states are included in the sum. That this is true for the condition used here will be become clear shortly.

The Dirac equation in the Z-string background has two regular short distant solutions and two irregular solutions. Denoting the regular short distance spinors by \vec{S}_i where $i = 1, 2$ then each of these will asymptotically match onto a unique linear combination of the asymptotic solutions given in (40),

$$\vec{S}_i \rightarrow \begin{pmatrix} J_{|\nu|}(\kappa) & 0 & N_{|\nu|}(\kappa) & 0 \\ \mp \frac{E}{k} J_{|\nu|\pm 1}(\kappa) & \mp \frac{q}{k} J_{|\nu|\pm 1}(\kappa) & \mp \frac{E}{k} N_{|\nu|\pm 1}(\kappa) & \mp \frac{q}{k} N_{|\nu|\pm 1}(\kappa) \\ 0 & J_{|\nu|}(\kappa) & 0 & N_{\nu}(\kappa) \\ \pm \frac{q}{k} J_{|\nu|\pm 1}(\kappa) & \pm \frac{E}{k} J_{|\nu|\pm 1}(\kappa) & \pm \frac{q}{k} N_{|\nu|\pm 1}(\kappa) & \pm \frac{E}{k} N_{|\nu|\pm 1}(\kappa) \end{pmatrix} \begin{pmatrix} a_{i,1} \\ a_{i,2} \\ a_{i,3} \\ a_{i,4} \end{pmatrix},$$

where, $\kappa = KR_o$, the upper sign corresponds to the case $|\nu| = \nu$ and the lower sign $|\nu| = -\nu$.

By taking an arbitrary linear combination of \vec{S}_1 and \vec{S}_2 and setting the 1st and 3rd components of the spinor to zero at $r = R_o$, we obtain the constraints,

$$\alpha(J_{|\nu|}(kR_o)a_{1,1} + N_{|\nu|}(kR_o)a_{1,3}) + \beta(J_{|\nu|}(kR_o)a_{2,1} + N_{|\nu|}(kR_o)a_{2,3}) = 0,$$

$$\alpha(J_{|\nu|}(kR_o)a_{1,2} + N_{|\nu|}(kR_o)a_{1,4}) + \beta(J_{|\nu|}(kR_o)a_{2,2} + N_{|\nu|}(kR_o)a_{2,4}) = 0,$$

from which it is easily seen that,

$$\frac{J_{|\nu|}(kR_o)}{N_{|\nu|}(kR_o)} = -\frac{(\alpha a_{1,3} + \beta a_{2,3})}{(\alpha a_{1,1} + \beta a_{2,1})} = -\frac{(\alpha a_{1,4} + \beta a_{2,4})}{(\alpha a_{1,2} + \beta a_{2,2})}. \quad (146)$$

Only the ratio $\gamma = \frac{\alpha}{\beta}$ is of interest and it is straightforward to derive the following quadratic equation for γ ,

$$A\gamma^2 + B\gamma + C = 0, \quad (147)$$

where,

$$A = a_{1,3}a_{1,2} - a_{1,1}a_{1,4}, \quad (148)$$

$$B = a_{1,3}a_{2,2} + a_{2,3}a_{1,2} - a_{1,1}a_{2,4} - a_{2,1}a_{1,4}, \quad (149)$$

$$C = a_{2,3}a_{2,2} - a_{2,1}a_{2,4}. \quad (150)$$

The solution to (147) can be substituted into (146) to produce two solutions for each particle,

$$\frac{J_{|\nu|}(kR_o)}{N_{|\nu|}(kR_o)} = -X^\pm(k), \quad (151)$$

where,

$$X^\pm(k) = \frac{(-B \pm \sqrt{B^2 - 4AC})a_{1,3} + 2Aa_{2,3}}{(-B \pm \sqrt{B^2 - 4AC})a_{1,1} + 2Aa_{2,1}}. \quad (152)$$

The left hand side of the discretisation condition is approximately $\cot(kR_o)$, thus for finite R_o there a discrete set of string states $\{k_i\}$ with $i \in \{1, 2, 3, \dots\}$ and spacing proportional to $\frac{1}{R_o}$. The density of the solutions becomes infinite as $R_o \rightarrow \infty$ and the full continuum is recovered.

It is possible to calculate the solutions of (51) numerically, for a fixed value of R_o and then compute the fermionic trace. The process can then be repeated for different values of R_o and the limit $R_o \rightarrow \infty$ taken numerically [24]. This is not the approach used here, instead the limit will be taken analytically. This saves the computation being repeated for different values of R_o .

For momentum k_i such that $k_i R_o \gg 1$, we can take the leading order asymptotic behaviour of the Bessel functions and write the discretisation condition as,

$$\cot(k_i R_o - \theta_\nu) = -X(k_i), \quad (153)$$

where,

$$\theta_\nu = \frac{\pi\nu}{2} + \frac{\pi}{4}.$$

This can be inverted to give,

$$k_i R_o = m(i)\pi + \theta_\nu + \cot^{-1}(-X(k_i)) \Big|_p, \quad (154)$$

where $|_p$ denotes the principle range of the inverse cotangent, throughout this is taken to be $[0, \pi]$. $m(i)$ is some integer valued function which specifies which branch of the cot function the solution lies on.

It is found that $X(k)$ is singular for certain values of k , the physical significance of such singularities is discussed in sections 8 and 9. A singularity in $X(k)$ corresponds to a discontinuity of π in the function $\cot^{-1}(-X(k))|_p$. As we take the limit the $R_o \rightarrow \infty$, the discrete set of solutions, $\{k_i\}$, tends towards a continuous spectrum. This continuum spectrum, as its name implies, is continuous in the momentum, thus the difference between consecutive elements of the set $\{k_i\}$ should tend to zero as the limit is taken. The requirement of continuity of the spectrum and the existence of singularities in $X(k)$ imply that some extra factor must be included. This extra function, $m(i)$, must jump in integer steps around the singularities of $X(k)$ to ensure that the spectrum defined by $\{k_i\}$ is indeed continuous as R_o is taken to ∞ .

It is convenient to write,

$$m(i) = i + \beta(i),$$

as this allows an evenly spaced free momentum k_i^o to be defined,

$$k_i^o R_o = i\pi.$$

The function $\beta(i)$ will be combined with the $\cot^{-1}(-X^\pm(k_i))|_p$ term to define a continuous function.

In regions where $X(k)$ is finite, we find one solution per branch of the cot function, thus $\beta(i)$ is a constant. However, if $X(k)$ is singular, there can be branches of the cot function with no solutions or two solutions (fig.1). We denote these singularities as Type 1 and Type 2 respectively.

Each branch of the function $\frac{J_{|\nu|}(kR_o)}{N_{|\nu|}(kR_o)}$ is bounded by two consecutive roots of $N_{|\nu|}(kR_o)$. Each solution of the discretisation condition lies along one of these branches and is thus bounded by two consecutive roots of $N_{|\nu|}(kR_o)$. Denoting the i th root of $N_\nu(kR_o)$ by σ_i^ν , the i th solution of (51) will satisfy the inequality,

$$\sigma_{i+\delta}^\nu < k_i R_o < \sigma_{i+1+\delta}^\nu, \quad (155)$$

where δ is an integer determined by the singularity structure of $X(k)$.

If $X^\pm(k)$ has no singularities, it is easy to see that the i th string state is bounded by the i th and the $(i+1)$ th roots of $N_\nu(kR_o)$ giving $\delta = 0$. A Type 1 singularity precludes a solution along one branch, thus above the singularity the i th solution is bounded by the $(i+1)$ th and $(i+2)$ th roots of $N_\nu(kR_o)$. In this case $\delta = 1$. Conversely, a Type 2 singularity gives two solutions on one branch. Thus above the singularity the i th solution is bounded by the $(i-1)$ th and the i th roots of $N_\nu(kR_o)$, giving $\delta = -1$.

By counting the singularities of each type, we can determine the value of δ at momenta greater than that of the highest momentum singularity of $X(k)$,

$$\delta = (\text{No. Type 1 Singularities} - \text{No. Type 2 Singularities}).$$

The asymptotic value of β , β_∞ , can then be set such that the solutions of the discretisation condition fall in the correct range. To leading order, the expansion for the large zeros of a Bessel function gives,

$$\sigma_m^\nu = \begin{cases} m\pi + \theta_\nu - \pi & \nu \geq 0 \\ m\pi + \theta_\nu - \pi + \text{int}[-\nu] & \nu < 0 \end{cases}$$

To place the high momentum solutions on the correct branches of the cot function we therefore set,

$$\beta_\infty = \delta - 1. \quad (156)$$

Having fixed the asymptotic value of β , we can now consider the effect of singularities in $X(k)$. Physically the occurrence of such singularities changes the number of continuum states which exist. It turns out that the singularities in the functions $X^\pm(k)$ are intimately linked to the bound state spectrum and they ensure that the total number of fermion states remains the same. The issue is covered in detail in section 8, where a specific model is used to demonstrate these points explicitly.

Consider first a Type 1 singularity. Denoting the the last solution of the discretisation condition before the singularity by $k_{i_s^-}$ and the first solution above the singularity by $k_{i_s^+}$, in the case of a Type 1 singularity we see (fig.1) that,

$$\cot^{-1}(-X(k_{i_s^-}))|_p \sim \pi, \quad (157)$$

and,

$$\cot^{-1}(-X(k_{i_s^+}))|_p \sim 0. \quad (158)$$

Using $i_{s^+} = i_{s^-} + 1$ and the discretisation condition (154), we see that,

$$(k_{i_{s^+}} - k_{i_{s^-}})R_o = O\left(\frac{1}{R_o}\right) + \beta(i_{s^+})\pi - \beta(i_{s^-})\pi. \quad (159)$$

As R_o becomes large we require that the momentum shifts are continuous, i.e. $(k_{i_{s^+}} - k_{i_{s^-}}) \sim \frac{\pi}{R_o}$. Thus we have a jump in β ;

$$\beta(i_{s^+}) = \beta(i_{s^-}) + 1. \quad (160)$$

This is precisely the jump expected due to a Type 1 singularity *skipping* a branch of the cot function. The singularity increases the value of δ by one, thus we expect β to increase by one. This jump ensures continuity of the discretisation condition about a Type 1 singularity. If we start at large momentum and work towards

small momentum, on passing the Type 1 singularity the inverse cotangent jumps upwards by π , but at exactly the same point the function $\beta(i)$ jumps down by π : hence there is no overall jump in the function and continuity across the singularity is ensured.

A similar analysis for a Type 2 singularity gives,

$$\beta(i_{s+}) = \beta(i_{s-}) - 1. \quad (161)$$

Again this jump is exactly that expected from a Type 2 singularity giving two solutions on one branch of the cot function, it ensures continuity of the discretisation condition around a Type 2 singularity.

It can be seen from (160) and (161) that the physical requirement of continuity in the spectrum arises naturally in this formulation.

Having fixed the discretisation condition uniquely for all values of the momentum the next step is to use the discretisation condition to formulate the regularised trace over the continuum states defined by (50). The manner in which the discretisation condition has been set up allows an integral over the continuum states to be defined in terms of the scattering data, found by solving the Dirac equation.

The discretisation condition can be written uniquely as,

$$k_i R_o = k_i^o R_o + \Delta^\pm(k_i), \quad (162)$$

where the free momentum is defined by,

$$k_i^o R_o = i\pi,$$

and,

$$\Delta^\pm(k) = \beta_\infty + \theta_\nu + \cot^{-1}(-X^\pm(k)) \Big|_p^{cont}, \quad (163)$$

where $i \in \{1, 2, \dots\}$ and $\cot^{-1}(-X^\pm(k)) \Big|_p^{cont}$ is continuous and takes the principal value for k larger than the last singularity in $X^\pm(k)$. It should be noted that for the pure Z-string there are two discretisation conditions of this type for each angular momentum mode labelled by \pm in (163). These arise from the two roots of the quadratic equation (147) which had to be solved in the process of setting up the discretisation condition for the Z-string background.

Appendix B: Computation of the Z-string Heat Kernel Coefficients

The purpose of this appendix is to provide details of the calculation of the coincidence limit heat kernel coefficients required for the computation of the counter term in the pure Z-string background.

$\text{Tr}[a_1]$. Using the standard recurrence relations we have,

$$\text{Tr}[a_1] = -a(x) = -4g^2 f^2(r) - 2iq(\alpha_L - \alpha_R)\partial_i Z_i + iq(\alpha_L - \alpha_R)\partial_i Z_j \text{Tr}\sigma^j \sigma^i. \quad (164)$$

Using the standard anti-commutation relation satisfied by the Pauli matrices, $\{\sigma^i, \sigma^j\} = 2\delta^{ij}$, gives, $Tr\sigma^i\sigma^j = 2\delta^{ij}$, hence the second and third terms in (164) cancel, leaving,

$$Tr[a_1] = -4g^2 f^2(r). \quad (165)$$

At this juncture it is however useful to note that individually the second and third terms in (164) vanish because the divergence of the gauge field in the string background is zero, that is $\partial_i Z_i = 0$, which is easily shown by direct calculation using (7).

$Tr[a_2]$. Again using the standard recurrence relations we find,

$$Tr[a_2] = \frac{1}{12} Tr\Gamma_{ij}\Gamma_{ij} + \frac{1}{2} Tra^2(x). \quad (166)$$

The first term in (166) is straightforward to compute: Γ_{ij} is the standard field strength tensor;

$$\Gamma_{ij} = \partial_i\Gamma_j - \partial_j\Gamma_i + [\Gamma_i, \Gamma_j]. \quad (167)$$

In the case of the pure Z-string the third term in (167) is zero because of the diagonal nature of Γ_i , hence,

$$\Gamma_{ij} = \partial_i\Gamma_j - \partial_j\Gamma_i = iqZ_{ij} \begin{pmatrix} \alpha_R & 0 \\ 0 & -\alpha_L \end{pmatrix}, \quad (168)$$

where,

$$Z_{ij} = \partial_i Z_j - \partial_j Z_i. \quad (169)$$

This is expected because the Z-string is really a Nielsen-Olesen $U(1)$ string embedded in the $U(1)_Z$ subgroup generated by the Z gauge bosons. Clearly Z_{ij} is anti-symmetric and so,

$$\Gamma_{ij}\Gamma_{ij} = -2q^2 Z_{12}^2 \begin{pmatrix} \alpha_R^2 & 0 \\ 0 & \alpha_L^2 \end{pmatrix}. \quad (170)$$

Using the specific forms of the gauge fields in the string background (7) implies that,

$$Z_{12} = -\frac{\nu'(r)}{r}, \quad (171)$$

and therefore,

$$Tr \Gamma_{ij}\Gamma_{ij} = -4(\alpha_R^2 + \alpha_L^2) \left(\frac{\nu'(r)}{r} \right)^2. \quad (172)$$

As we only need its trace, only the diagonal elements of $a(x)^2$ need to be considered. Using $\partial_i Z_i = 0$, it can be shown that,

$$\begin{aligned} Tra(x)^2 &= 4g^4 f(r)^4 - q^2(\alpha_L^2 + \alpha_R^2) Tr(\sigma^j \sigma^i \partial_i Z_j)^2 \\ &\quad + 2g^2 \partial_i (f(r)e^{\pm i\theta}) \partial_i (f(r)e^{\mp i\theta}) \\ &\quad + 2q^2 g^2 f(r)^2 Z_i Z_i \\ &\quad \pm 2iqg^2 f(r) Z_j \left(e^{\pm i\theta} \partial_i (f(r)e^{\mp i\theta}) - e^{\mp i\theta} \partial_i (f(r)e^{\pm i\theta}) \right). \end{aligned} \quad (173)$$

Now the explicit forms of the gauge fields given in (7) can be substituted into (173). The computation is straightforward but it is useful to give the explicit forms of some of the individual terms which appear in (173),

$$Z_i Z_i = \left(\frac{\nu(r)}{qr} \right)^2, \quad (174)$$

$$\sigma^j \sigma^i \partial_i Z_j = -i \frac{\nu'(r)}{qr} \sigma^3, \quad (175)$$

$$\sigma^i \partial_i (f(r) e^{\pm i\theta}) = \begin{pmatrix} 0 & e^{-i\theta} \\ e^{i\theta} & 0 \end{pmatrix} e^{\pm i\theta} f'(r) \pm \begin{pmatrix} 0 & e^{-i\theta} \\ -e^{i\theta} & 0 \end{pmatrix} e^{\pm i\theta} \left(\frac{f(r)}{r} \right), \quad (176)$$

$$Z_i e^{\pm i\theta} \partial_i (f(r) e^{\mp i\theta}) = \mp i \frac{\nu(r) f(r)}{qr^2}. \quad (177)$$

Using (174) to (177) in (173) gives the required expression for $\text{Tr } a(x)^2$ expressed purely in terms of the Nielsen-Olesen profile functions and the parameters in the theory. After a little algebra it can be shown that,

$$\begin{aligned} \text{Tr } a(x)^2 &= 2g^4 f(r)^4 + \frac{2}{3} (\alpha_R^2 + \alpha_L^2) \left(\frac{\nu(r)'}{r} \right)^2 \\ &\quad + 2g^2 \left((f'(r))^2 + \left(\frac{f(r)}{r} \right)^2 \right) \\ &\quad + 2g^2 \frac{f(r)^2 \nu(r)^2}{r^2} + 4g^2 \frac{f(r)^2 \nu(r)}{r^2}. \end{aligned} \quad (178)$$

It is then easy to show by direct substitution of (172) and (178) into (166) that the expression for $\text{Tr}[a_1]$ is indeed that given by (65).